Molecular Pharmacology Fast Forward. Published on December 22, 2014 as DOI: 10.1124/mol.114.096065
This article has not been copyedited and formatted. The final version may differ from this version.

MOLPHARM/2014/96065

The c-MET/PI3K signaling is associated with cancer resistance to doxorubicin and photodynamic therapy by elevating BCRP/ABCG2 expression

Kyeong-Ah Jung, Bo-hyun Choi, and Mi-Kyoung Kwak

College of Pharmacy, The Catholic University of Korea, Bucheon, Gyeonggi-do 420-743, Republic of Korea

Molecular Pharmacology Fast Forward. Published on December 22, 2014 as DOI: 10.1124/mol.114.096065
This article has not been copyedited and formatted. The final version may differ from this version.

Running Title: Role of c-MET/BCRP signaling in cancer resistance

Corresponding author: M-K Kwak

College of Pharmacy, The Catholic University of Korea, 43 Jibong-ro, Wonmi-gu, Bucheon, Gyeonggi-do 420-743, Republic of Korea, E-mail: mkwak@catholic.ac.kr

Document statistics:

42 pages

1 table

8 figures

1 supplemental table and 2 supplemental figures

244 words in abstract

1,132 words in introduction

1,547 words in discussion

Abbreviations:

A2780DR, doxorubicin resistant A2780 cell line; Pba, pheophorbide a; BCRP/ABCG2, breast cancer resistance protein; MRP/ABCC, multidrug resistance protein; MDR/ABCB1, multidrug resistance protein; PI, propidium iodide; CMF-DA, 5-chloromethylfluorescein diacetate; DCFDA, trans-1-(2'-methoxyvinyl)pyrene, carboxy-2′,7′-dichlorofluorescein diacetate; ROS, reactive oxygen species; MTT, 3-(4, 5-dimethylthiazonl-2-yl)-2,5-diphenyltetrazolium bromide; HGF, hepatocyte growth factor; PI3K, phosphoinositide 3-kinase; Dox, doxorubicin; H342, Hoechst 33342; LY294, LY294002; SU112, SU11274

Molecular Pharmacology Fast Forward. Published on December 22, 2014 as DOI: 10.1124/mol.114.096065
This article has not been copyedited and formatted. The final version may differ from this version.

Abstract

Overexpression of BCRP/ABCG2, a xenobiotic efflux transporter, is associated with anticancer drug resistance in tumors. Proto-oncogene c-MET induces cancer cell proliferation, motility, and survival, and its aberrant activation was found to be a prognostic factor in advanced ovarian cancers. In the present study, we investigated the potential cross-resistance of doxorubicin-resistant ovarian cancer cells to the pheophorbide a (Pba)-based photodynamic therapy (PDT), and suggest c-MET and BCRP/ABCG2 overexpression as an underlying molecular mechanism. A2780DR, which was established by incubating A2780 with stepwise increasing concentrations of doxorubicin, showed low levels of cellular Pba accumulation and ROS generation, and was more resistant to PDT cytotoxicity than A2780. In a microarray analysis, BCRP/ABCG2 was found to be the only drug transporter whose expression was up-regulated in A2780DR; this increase was confirmed by western blot and immunocytochemical analyses. As functional evidence, the treatment with a BCRP/ABCG2-specific inhibitor reversed A2780DR resistance to both doxorubicin and PDT. We identified that c-MET increase is related to BCRP/ABCG2 activation. The c-MET downstream PI3K/AKT signaling was activated in A2780DR and the inhibition of PI3K/AKT or c-MET repressed resistance to doxorubicin and PDT. Finally, we showed that the pharmacological and genetic inhibition of c-MET diminished levels of BCRP/ABCG2 in A2780DR. Moreover, c-MET inhibition could repress BCRP/ABCG2 expression in breast carcinoma MDA-MB-231 and colon carcinoma HT29, resulting in sensitization to doxorubicin. Collectively, our results provide a novel link of c-MET overexpression to BCRP/ABCG2 activation, suggesting that this mechanism leads to cross-resistance to both chemotherapy and PDT.

Molecular Pharmacology Fast Forward. Published on December 22, 2014 as DOI: 10.1124/mol.114.096065
This article has not been copyedited and formatted. The final version may differ from this version.

Introduction

The anthracycline antibiotic doxorubicin (adriamycin) is an effective drug for the treatment of a variety of solid tumors including ovarian cancer. Although its activity is not fully understood, it has been known that doxorubicin induces apoptosis in cancer by DNA intercalation, inhibition of DNA synthesis, and reactive oxygen species (ROS) generation (Minotti et al., 2004; Muller et al., 1998). Due to a dose-limiting cardiotoxicity, the development of doxorubicin resistance can finally cause treatment failure. Cellular defects, including p53 loss and death receptor impairment are related to poor therapeutic response to courses of doxorubicin treatment (Muller et al., 1998). In addition, increased expression of drug efflux transporters, such as multidrug resistance protein-1 (MDR1/ABCB1) and breast cancer resistant protein (BCRP/ABCG2), has been observed in refractory tumors (Jamieson and Boddy, 2011).

Photodynamic therapy (PDT) has been approved worldwide as an alternative treatment modality for several types of cancer (Dolmans et al., 2003; Dougherty et al., 1998; Hopper, 2000). In PDT, a photosensitizer within tumor tissue is activated by light irradiation, generating singlet oxygen ($^1O_2$) by transferring energy to adjacent molecular oxygen. In addition, it has been reported that the activated photosensitizer can directly produce ROS by reacting with oxygen. Because singlet oxygen and ROS are damaging to cellular components, targeted cancer cells undergo apoptotic or necrotic cell death (Buytaert et al., 2007; Sharman et al., 2000). In a clinical setting, the use of PDT is largely limited to superficial tumors because the wavelengths of light used in PDT cannot penetrate the body. Pheophorbide-A (Pba) is a chlorophyll derivative from silkworm excreta and the Chinese medicinal herb *Scutellaria barbarta* (Chan et al., 2006; Park et al., 1989). Unlike two FDA-approved

Molecular Pharmacology Fast Forward. Published on December 22, 2014 as DOI: 10.1124/mol.114.096065
This article has not been copyedited and formatted. The final version may differ from this version.

photosensitizers Photofrin and Levulan (5-aminolevulinic acid), Pba can be excited by a longer wavelength of light, enabling enhanced penetration into peritoneal cavity-located tumors like ovarian cancer (Xodo et al., 2012). Pba was shown to cause mitochondria-dependent apoptosis in cultured cancer cells (Tang et al., 2009). *In vivo* animal models also demonstrated that Pba impedes tumor growth in colon carcinoma and hepatoma xenograft models (Hajri et al., 2002; Li et al., 2007). However, the development of PDT resistance has been displayed: colon cancer cells repeatedly exposed to PDT agents developed resistance to PDT (Singh et al., 2001). Although there are many discordant reports, cross-resistance between PDT and chemotherapy has been suggested. Fibrosarcoma cells resistant to Photofrin-PDT showed low levels of cisplatin cytotoxicity and cisplatin-DNA adduct formation (Moorehead et al., 1994).

ATP-binding cassette (ABC) transporters such as BCRP/ABCG2 control the active efflux of intracellular xenobiotic chemicals through the plasma membrane (Jamieson and Boddy, 2011; Stacy et al., 2013). The active form of BCRP/ABCG2 is a homodimer (140 kDa) located in the plasma membrane. BCRP/ABCG2 was first reported as a xenobiotic transporter in a multidrug resistant human breast cancer cell line (Doyle et al., 1998). After this, it was revealed that BCRP/ABCG2 overexpression is responsible for drug resistance to anticancer doxorubicin, mitoxantrone, and topotecan (Litman et al., 2000). In addition, increased BCRP/ABCG2 expression was negatively correlated with accumulation of porphyrin-type photosensitizers like Pba and protoporphyrin IX (Robey et al., 2005), which leads to the poor responsiveness to PDT. The involvement of several response elements in the 5'-flanking region has been suggested as an underlying mechanism of BCRP/ABCG2 expression control. These regulating sequences include response elements for peroxisome

Molecular Pharmacology Fast Forward. Published on December 22, 2014 as DOI: 10.1124/mol.114.096065
This article has not been copyedited and formatted. The final version may differ from this version.

proliferator-activated receptor (PPAR), hypoxia, and progesterone (An and Ongkeko, 2009). Overexpression of PPARγ was shown to elevate BCRP/ABCG2 expression in human dendritic cells (Szatmari et al., 2006). The incubation of human placental cells with progesterone and estradiol increased BCRP/ABCG2 expression via the progesterone receptor (Wang et al., 2006). Binding of the hypoxia-inducible factor 1α (HIF1α) to the *BCRP* promoter increased BCRP/ABCG2 gene transcription, implying the association of BCRP/ABCG2 overexpression within tumors (Krishnamurthy et al., 2004). The *tert*-butylhydroquinone-inducible BCRP/ABCG2 expression was mediated through NF-E2-related factor 2 (NRF2) in HepG2 cells (Adachi et al., 2007).

The receptor tyrosine kinase c-MET is primarily expressed in epithelial and endothelial cells. It transduces signaling from hepatocyte growth factor (HGF) primarily produced by mesenchymal and stromal cells (Ghiso and Giordano, 2013; Graveel et al., 2013). HGF/c-MET signaling has been associated with the oncogenesis of various cancers by enhancing cell proliferation, motility, and survival. The expression of c-MET is highly elevated in lung, prostate, and ovarian cancers; high expression levels are strongly associated with poor prognosis (Humphrey et al., 1995; Ichimura et al., 1996; Sawada et al., 2007). Upon stimulation, the autophosphorylation of c-Met homodimer mediates downstream signaling via multiple molecular pathways, including the mitogen-activated protein kinases (MAPKs), phosphatidylinositol-4,5-bisphosphate 3-kinase (PI3K)-AKT, and signal transducer and activator of transcription (STAT) (Ghiso and Giordano, 2013; Graveel et al., 2013).

In this report, we investigated the development of potential cross-resistance between chemotherapy and PDT using the ovarian carcinoma A2780DR, a cell line that has acquired

adaptive resistance to doxorubicin. A2780DR exhibits resistance to Pba-based PDT when compared to its parent cell line A2780. Cellular Pba accumulation, ROS generation, and cytotoxicity of Pba-based PDT are lowered in A2780DR. We show that the elevated level of BCRP/ABCG2 is responsible for A2780DR resistance to doxorubicin and PDT. Further analyses with microarrays and pharmacological inhibitors revealed that c-MET overexpression and resultant activation of the PI3K/AKT signaling cascade is involved in increased expression of BCRP/ABCG2 and cross-resistance to doxorubicin and PDT.

Material and methods

Materials

Pba was obtained from Santa Cruz Biotechnology (Santa Cruz, CA, USA). Doxorubicin, Ko143, LY294002 (LY294), SU11274 (SU112), propidium iodide (PI), 3-(4,5-dimethylthiazol-2-yl)-2,5-diphenyltetrazolium bromide (MTT), and puromycin were purchased from Sigma-Aldrich (Saint Louis, MO, USA). Hoechst 33342 (H342), trans-1-(2'-methoxyvinyl)pyrene, carboxy-2′,7′-dichlorofluorescein diacetate (DCF-DA), Alexa Fluor® 488 goat anti-rabbit IgG (H+L) were purchased from Life Technologies (Carlsbad, CA, USA). The SYBR premix ExTaq system was obtained from Takara (Otsu, Japan). Antibodies recognizing c-MET, PI3K (p85α), AKT, p-AKT, and BCRP/ABCG2 were obtained from Cell Signaling Technology (Danvers, MA, USA). β-Tubulin antibody was purchased from Santa Cruz Biotechnology. Cisplatin and 5-fluorouracil (5-FU) were purchased from Sigma-Aldrich. Paclitaxel was obtained from MedKoo Biosciences (Chapel Hill, NC, USA).

Molecular Pharmacology Fast Forward. Published on December 22, 2014 as DOI: 10.1124/mol.114.096065
This article has not been copyedited and formatted. The final version may differ from this version.

Cell culture

Human ovarian cancer cell line A2780 was purchased from the European Collection of Cell Cultures (Salisbury, Wiltshire, UK). Doxorubicin resistant A2780 cell line (A2780DR) was established in our previous study (Shim et al., 2009). These cells were maintained in RPMI 1640 (Hyclone, Logan, UT, USA) with 10% fetal bovine serum (Hyclone) and 1% penicillin/streptomycin (WelGene Inc., Daegu, South Korea). The human breast cancer cell line MDA-MB-231 and colon cancer cell line HT29 were obtained from American Type Culture Collection (Rockville, MD, USA). MDA-MB-231 was maintained in a medium containing Dulbecco's Modified Eagle Medium (Hyclone). HT29 was maintained in RPMI-1640 medium. The cells were grown at 37 °C in a humidified 5 % CO_2 atmosphere.

PDT treatment

A2870 and A2780DR were plated at a density of 5×10^3 cells/well in 96-well plates and after 24 h, PDT was performed as described in the previous study (Choi et al., 2014). Briefly, the cells were treated with Pba (0.025 – 2.5 μg/ml) for 6 h, and then Pba-containing medium was removed. The 670 nm LED Hybrid Lamp system (Quantum Spectra Life®, Barneveld, WI) was used to irradiate the cells with 1.2 J/cm² laser. Then the cells were recovered in a complete medium for 18 h for further analyses.

MTT analysis

Cells were plated at a density of 3×103 cells/well in 96-well plates. After the treatment with PDT or anticancer agents, MTT solution (2 mg/ml) was incubated for 4 h. MTT solution was removed and 100 μl of dimethyl sulfoxide (DMSO) was added to each

Molecular Pharmacology Fast Forward. Published on December 22, 2014 as DOI: 10.1124/mol.114.096065
This article has not been copyedited and formatted. The final version may differ from this version.

well. The absorbance was measured at 570 nm using a Spectro-star Nano microplate reader (BMG Lab Technologies, Offenburg, Germany).

Measurement of reactive oxygen species (ROS)

Cells were plated at a density of 7×10^3 cells/well on a cover glass slide (SPL Life Sciences, Gyeonggi-do, Korea). After PDT, the cells were washed with PBS and incubated with trans-1(2'-methoxyvinyl)pyrene (50 μM) or DCF-DA (30 μM) at 37 °C as previously described (Choi et al., 2014). Fluorescent images were obtained using an appropriate filter (488/524 nm) in a LSM 710 confocal microscope (Carl Zeiss, Jena, Germany) and intensities were quantified using the ZEN2011 software (Carl Zeiss). To analyze cellular fluorescence images using a Cell Insight™ Personal Cell Imager (Thermo Fisher Scientific, Waltham, MA, USA) cells were seeded in 96-well plates and ROS-generated fluorescent images (495/529 nm) were quantified following nuclear staining with H342 (350/461 nm).

Measurement of intracellular accumulation of doxorubicin and Pba

The cells were plated at a density of 7×10^3 cells on cover glass slides and incubated with doxorubicin or Pba for 6 h. Then, doxorubicin or Pba was removed and PBS washes were followed. Intensities of cellular red fluorescence from doxorubicin (548/680 nm) or Pba (633/693 nm) were obtained using a LSM 710 confocal microscope. As an alternative way for quantification, cells were seeded in 96-well plates and incubated with doxorubicin or Pba. After the cell wash and nuclear staining, red fluorescence was detected using a Cell Insight™ Personal Cell Imager and intensities were quantified with corresponding software.

Molecular Pharmacology Fast Forward. Published on December 22, 2014 as DOI: 10.1124/mol.114.096065
This article has not been copyedited and formatted. The final version may differ from this version.

Fluorometric determination of intracellular Pba

Cells in 96-well plates were incubated with Pba for 6 h and then lysed using 1% SDS after PBS wash. DMSO was added to cell lysates to dissolve cellular Pba and fluorescence intensity measured using a SpectraMax M5 (415 nm Ex /673 nm Em).

Total RNA extraction and real time RT-PCR analysis

The total RNAs were isolated from the cells using a TRIzol reagent (Life Technologies). For the synthesis of cDNA, reverse-transcriptase (RT) reactions were performed by incubating 200 ng of the total RNAs with a reaction mixture containing 0.5 μg/μl oligo dT_{15} (Promega, Madison, WI, USA) and reverse transcriptase (Promega). For relative quantification of mRNA levels the real-time polymerase-chain reaction (PCR) analysis was performed using a Roche LightCycler (Roche, Mannheim, Germany) with SYBR Premix ExTaq system. Each primer was synthesized by Bioneer (Daejeon, South Korea). The sequences of forward and reverse primers for human genes are as follows: *MDR1/ABCB1*, 5′-CTATGCTGGATGTTTCCGGT-3′ and 5′-TCTTCACCTGGCTCAGT-3′; *MRP1/ABCC1*; 5’-AGCTTTATGCCTGGGAGCTGGC-3’ and 5’-CGGCAAATGTGCACAAGGCCAC-3’; *MRP2/ABCC2*, 5’-GCTGCCACACTTCAGGCTCT-3’ and 5’-GGCAGCCAGCAGTGAAAGC-3’; *BCRP/ABCG2*, 5’-CACAACCATTGCATCTTGGCTG-3’ and 5’-TGAGAGATCGATGCCCTGCTTT-3’; *HGF*, 5’-ACAGCTTTTTGCCTTCGAGC-3’ and 5’-TAACTCTCCCCATTGCAGGT-3’; *c-MET*, 5’-TATGTGGCTGGGACTTTGGA-3’ and 5’-GCTTATTCATGGCAGGACCAAC-3’.

Molecular Pharmacology Fast Forward. Published on December 22, 2014 as DOI: 10.1124/mol.114.096065
This article has not been copyedited and formatted. The final version may differ from this version.

Microarray analysis

Total RNAs were isolated from A2780 and A2780DR cells using the Totally RNA Kit (Ambion, Austin, TX, USA) and further purified w the RNeasy Mini kit (Qiagen, Valencia, CA, USA). The RNAs were used for cDNA synthesis and cRNA labeling (Enzo Biochemical, Farmingdale, NY, USA). Then fragmented cRNAs (12.5 μg) were hybridized to a Human Gene ST array (HuGene-1-0-ST-v1; Affymetrix, Santa Clara, CA, USA) at 45 °C for 16 h. Data were generated using GenPlex version 3.0 software (ISTECH, South Korea).

Western blot analysis

Cells were lysed with lysis buffer (50 mM Tris [pH 7.4], 150 mM NaCl, 1 mM EDTA, and 1% nonyl phenoxypolyethoxylethanol 40) containing a protease inhibitor cocktail (Sigma-Aldrich). The protein concentration was determined using a BCA protein kit (Thermo Scientific). Obtained protein samples were separated by electrophoresis on 8-12 % SDS-polyacrylamide gels and transferred to nitrocellulose membranes (Whatman GmbH, Dassel, Germany). The membrane was then blocked with 5% skim milk or 3% BSA for 1 h and then incubated with corresponding primary antibody overnight. After washing with tween 20-containing PBS, the membrane was incubated with a secondary antibody for 1 h. The chemiluminescent images were captured using an ImageQuant LAS 4000 Mini (GE Healthcare Life Sciences, Piscataway, NJ, USA).

Immunocytochemical analysis

Cells were plated at a density of 7×10^3 cells/well on cover glass slides and drug treatment was initiated. The cells were washed with cold PBS three times and were fixed in

Molecular Pharmacology Fast Forward. Published on December 22, 2014 as DOI: 10.1124/mol.114.096065
This article has not been copyedited and formatted. The final version may differ from this version.

cold methanol for 10 min. Then, anti-BCPR/ABCG2 (1:200) antibody was incubated in fixed cells at 4°C overnight. Next day, the cells were washed with PBS and the Alexa Fluor® 488 goat anti-rabbit antibody (1:500) incubation was performed at room temperature for 1 h. For nuclear staining, PI (1:250) incubation was executed for 10 min. Fluorescent images were obtained using a LSM 710 confocal microscopy.

c-MET siRNA transfection

Predesigned c-MET siRNA (#51, 5'-GUGAAGAUCCCAUUGUCUA-3' and 5'-UAGACAAUGGGAUCUUCAC-3') and a scrambled (sc) control siRNA were obtained from Bioneer. The cells were seeded in 60 mm plates at a density of 5×10^4 cells and grown overnight. Next day, cells were transfected with c-MET siRNA using a Lipofectamine 2000 reagent (Life Technologies). RNAs and proteins were extracted after recovery for 24 h in complete medium.

Statistical analysis

Statistical significance was determined by a Student paired t-test followed or a one-way analysis of variance (one-way ANOVA) followed by the Student Newman–Keuls test for multiple comparisons using GraphPad Prism software (La Jolla CA, USA).

Results

A2780DR was more resistant to doxorubicin accumulation and PDT cytotoxicity than A2780

The A2780DR cell line was established by maintaining human ovarian carcinoma A2780 cells in doxorubicin-containing medium (Shim et al., 2009). When A2780 and

Molecular Pharmacology Fast Forward. Published on December 22, 2014 as DOI: 10.1124/mol.114.096065
This article has not been copyedited and formatted. The final version may differ from this version.

A2780DR cells were incubated with doxorubicin (0.2-1.6 μM) for 72 h, A2780DR cells showed much higher viability than the parental A2780 cells (Fig. 1A). The anthracycline chromophore group in doxorubicin is also a fluorophore; therefore, cellular accumulation of doxorubicin can be visualized and quantified using a fluorescent cell imager. Incubation with doxorubicin increased level of cellular fluorescence in a concentration-dependent manner (1-4 μM) in both cell lines, however, the magnitude of increase is significantly smaller in A2780DR cells (Fig. 1B). The cellular doxorubicin level increased up to 11-fold following 4 μM doxorubicin incubation for 6 h in A2780, whereas only a 5.5-fold increase was observed in A2780DR. Whereas, the A2780DR sensitivity to other anticancer drugs such as cisplatin, paclitaxel, and 5-fluorouracil was not significantly different from A2780, suggesting that doxorubicin resistance of A2780DR was developed through a specific mechanism (Supplementary Fig. S1).

PDT has been approved as an effective treatment option for various solid tumors. The identification of molecular determinants of the responsiveness of PDT is necessary to optimize the therapeutic effect of PDT. In this aspect, we hypothesized that doxorubicin resistant A2780DR cells may have differential susceptibility to PDT and investigated the responsiveness of A2780DR to Pba-based PDT. MTT analysis showed that incubation with Pba (24 h) up to 2.5 μg/ml did not affect cell viability in both A2780 and A2780DR (Fig. 1C). When Pba-incubated A2780 was irradiated with laser light for 60 s, the viable cell number was decreased in a concentration-dependent manner; only 25% and 14% cells survived following PDT with 0.125 and 0.25 μg/ml Pba respectively (Fig. 1D). A2780DR was clearly resistant to PDT cytotoxicity: 83% cells were viable following 0.25 μg/ml Pba-PDT. These results indicate that A2780DR is cross-resistant to doxorubicin and Pba-PDT.

Molecular Pharmacology Fast Forward. Published on December 22, 2014 as DOI: 10.1124/mol.114.096065
This article has not been copyedited and formatted. The final version may differ from this version.

PDT-induced ROS increase and cellular Pba accumulation were mitigated in A2780DR

Levels of cytotoxic oxygen species were significantly lower following PDT in A2780DR than in A2780. The incubation of cells with singlet oxygen-specific dye showed an increase in green fluorescence right after laser irradiation in A2780. Fluorescence intensity was elevated by 1.3-fold and 1.6-fold in the 0.25 and 2.5 μg/ml group, respectively (Fig. 2A), whereas the in the presence of singlet oxygen was significantly lower in A2780DR. Similarly, PDT-treated A2780 exhibited a high level of cellular ROS not observed in A2780DR (Fig. 2B). These findings support reduced cytotoxic responsiveness of A2780DR to PDT. In particular, it was notable that generated singlet oxygen level is low in A2780DR, which implies that the cellular level of photosensitizer Pba might be differential. Following Pba incubation for 6 h, cellular red fluorescence intensities derived from Pba were elevated by 28-fold in A2780 with 2.5 μg/ml Pba. On the other hand, A2780DR cells accumulated less Pba: the fluorescent intensity increase was 10.5-fold in 2.5 μg/ml Pba (Fig. 2C). When the cell lysates from the lower concentrations of Pba (0.25, 0.5, and 1 μg/ml)-incubated cells were measured with fluorometry, similar differences were observed (Supplementary Fig. S2). These results indicate that PDT susceptibility is low in doxorubicin-resistant ovarian cancer cells and this phenomenon is associated with a diminished cellular level of Pba.

BCRP/ABCG2 activation-induced doxorubicin resistance in A2780DR

The efflux of cellular doxorubicin is mediated by ABC transporters such as MDR1/ABCB1, BCRP/ABCG2/ABCG2, and MRP1/ABCC1 (Jamieson and Boddy, 2011). In an attempt to elucidate the causative reason of lower cellular levels of doxorubicin and Pba, the transporter expression pattern of A2780DR was compared to that of A2780. It is

Molecular Pharmacology Fast Forward. Published on December 22, 2014 as DOI: 10.1124/mol.114.096065
This article has not been copyedited and formatted. The final version may differ from this version.

especially notable that BCRP/ABCG2 was the only gene among the 50 sampled ABC transporters in which expression is elevated more than 50% in A2780DR. The transcript level of BCRP/ABCG2 was 45-fold higher in A2780DR as compared to A2780 (Table 1).

When transcript levels for BCRP/ABCG2, MDR1/ABCB1, and MRP1~2/ABCC1~2 were determined using real time RT-PCR analysis, the BCRP/ABCG2 mRNA level was 71 times higher in A2780DR, implicating its potential role in differential Pba accumulation (Fig. 3A). Similarly, the western blot analysis showed that the protein level of BCRP/ABCG2 was substantially higher in A2780DR compared to A2780 (Fig. 3B). In addition, immunocytochemical analysis showed that elevated BCRP/ABCG2 expression is largely located in the plasma membrane in A2780DR (Fig. 3C). Functional implications of increased expression of BCRP/ABCG2 can be confirmed by cellular staining with H342, a substrate of BCRP/ABCG2. A2780 showed nuclear staining following H342 dye incubation for 10 min, whereas A2780DR displayed extracellular accumulation of H342 resulting in low cellular level (Fig. 3D). Differential distribution of H342 was abolished by incubation with the BCRP/ABCG2-specific inhibitor Ko143, confirming the predominant role of BCRP/ABCG2 in H342 transport (Data not shown). Whereas, cellular levels of CMF-DA, a substrate of MRP/ABCC, were similar in both cell lines (Fig. 3E).

Finally, BCRP/ABCG2 expression was strongly associated with differential doxorubicin accumulation: the reduced cellular levels of doxorubicin in A2780DR were completely restored to that of A2780 by incubation with BCRP/ABCG2 inhibitor Ko143 (Fig. 3F). Consistently, pretreatment of Ko143 diminished viable cell numbers in A2780DR following doxorubicin treatment (Data not shown). Collectively, these results show that BCRP/ABCG2 expression is distinctly elevated during the acquisition of doxorubicin

Molecular Pharmacology Fast Forward. Published on December 22, 2014 as DOI: 10.1124/mol.114.096065
This article has not been copyedited and formatted. The final version may differ from this version.

resistance in A2780, and this mechanism, in turn, leads to the attenuation of doxorubicin accumulation in resistant cells.

BCRP/ABCG2 activation was responsible for reduced Pba responsiveness in A2780DR

In order to clarify whether elevated BCRP/ABCG2 expression is responsible for PDT resistance of A2780DR, we first monitored cellular Pba levels following BCRP/ABCG2 inhibitor treatment. Lower levels of Pba (0.25 and 2.5 μg/ml) in A2780DR were completely recovered to those of A2780 following Ko143 pre-incubation (Fig. 4A). The pre-treatment of A2780DR with MK-571, a specific inhibitor of MRPs, did not alter Pba accumulation, however, confirming the predominant role of BCRP/ABCG2 in Pba transport (Data not shown). Ko143 pre-treatment was shown to elevate PDT-stimulated singlet oxygen levels in A2780DR (1.38-fold to 2.35-fold), but not in A2780 (Fig. 4B). The increase in PDT cell viability in A2780DR was concordantly blocked by Ko143 treatment (Fig. 4C). These results indicate that increased BCRP/ABCG2 function in A2780DR leads to enhanced extracellular export of Pba and thus consequent protection against PDT cytotoxicity.

c-MET overexpression in A2780DR and its association with doxorubicin resistance

Based on obtained results showing the overexpression of BCRP/ABCG2 and consequent resistance to PDT and doxorubicin treatment in A2780DR, we next attempted to identify underlying molecular mechanisms of BCRP/ABCG2 increase. It is particularly notable that the expression of proto-oncogene c-MET is relatively high in A2780DR when compared to that of its parental A2780 cells (Supplementary Table S1). c-MET transduces a signal to the PI3K/AKT pathway for enhanced tumor growth, migration, and survival

Molecular Pharmacology Fast Forward. Published on December 22, 2014 as DOI: 10.1124/mol.114.096065
This article has not been copyedited and formatted. The final version may differ from this version.

(Graveel et al., 2013), and A2780 has been reported to express very low levels of c-MET (Sawada et al., 2007). The transcript level of c-MET in A2780DR was found to be 3.6-fold higher in microarray analysis (Supplementary Table S1) and a similar increase was confirmed in real time RT-PCR analysis (Fig. 5A). Nonetheless, there were no significance differences in transcript levels for HGF, AKT, catalytic subunits of PI3K, and phosphatase and tensin homolog (PTEN) between A2780DR and A2780. Only PI3K regulatory subunit-1 (p85) was increased by 1.92-fold (Supplementary Table S1). In western blot analysis, A2780DR cells showed increased levels of c-MET (145 kDa) in A2780DR (Fig. 5B). With a similar pattern observed in microarray analysis, the level p85 subunit of PI3K was marginally elevated in A2780DR. Moreover, the protein level of phosphorylated AKT, a downstream of activated PI3K, was substantially high in A2780DR cells, confirming the activation of c-MET/PI3K/AKT signaling in these cells.

Since there are previous reports showing that the activation of PI3K/AKT signaling can up-regulate BCRP/ABCG2 activity (An and Ongkeko, 2009; Mogi et al., 2003), elevated c-MET expression may be involved in increased expression of BCRP/ABCG2 in A2780DR. This potential relationship can be supported by the effects of pharmacological inhibitors of PI3K and c-MET. After pre-incubation of A2780DR with PI3K-specific inhibitor LY294002 (LY294; 5 or 10 μM) for 3 h, cellular levels of doxorubicin increased to the levels of A2780 (Fig. 5C). Similarly, when A2780DR was pre-treated with c-MET-specific tyrosine kinase inhibitor SU11274 (SU112; 1 or 2 μM) for 3 h, the intracellular level of doxorubicin increased by 50% (Fig. 5D). In addition, A2780DR resistance to doxorubicin was significantly attenuated by SU114 (Fig. 5E). These results suggest that elevated c-MET/PI3K signaling may be responsible for suppressed doxorubicin accumulation in A2780DR.

Molecular Pharmacology Fast Forward. Published on December 22, 2014 as DOI: 10.1124/mol.114.096065
This article has not been copyedited and formatted. The final version may differ from this version.

c-MET/PI3K/AKT signaling was related with PDT resistance of A2780DR

To investigate the role of c-MET/PI3K signaling in A2780DR PDT resistance, we examined the effects of pharmacological inhibitors on PDT cytotoxicity, singlet oxygen levels, and Pba accumulation. When cells were pre-incubated in LY294 (5 μM), the level of accumulated Pba was enhanced in A2780DR but not in A2780 (Fig. 6A). In addition, level of singlet oxygen in A2780DR was increased to the level of A2780 (Fig. 6B). Finally, PDT cell viability was affected by PI3K inhibition in A2780DR; the percentage of viable cells decreased from 76% to 31% by LY294 incubation (Fig. 6C).

Next, the PDT response of cells pre-treated with the c-MET-specific inhibitor SU112 (1 μM) was assessed. The c-MET inhibitor incubation restored intracellular accumulation of Pba (Fig. 6D) and elevated singlet oxygen level only in A2780DR (Fig. 6E). Accordantly, the cell viability of A2780DR decreased from 62% to 33% following PDT (Fig. 6F). These results indicate that increased c-MET expression and subsequent PI3K signaling is strongly associated with PDT resistance in A2780DR.

c-MET increase in A2780DR was linked to BCRP/ABCG2 overexpression

The involvement of c-MET/PI3K signaling in BCRP/ABCG2 expression was asked by monitoring levels of c-MET, PI3K, AKT, and BCRP/ABCG2 following treatment with pharmacological inhibitors. First, when cells were incubated with the PI3K inhibitor LY294 (5 μM) for 3, 6, and 24 h, levels of p-AKT were decreased in A2780DR, confirming the effect of the inhibitor (Fig. 7A). Notably, elevated levels of BCRP/ABCG2 monomer in A2780DR were diminished by LY294 in a time-dependent manner. An immunocytochemical analysis also confirmed a decrease of BCRP/ABCG2 expression in A2780DR;

Molecular Pharmacology Fast Forward. Published on December 22, 2014 as DOI: 10.1124/mol.114.096065
This article has not been copyedited and formatted. The final version may differ from this version.

BCRP/ABCG2-positive fluorescent intensities were diminished by 3 h of incubation (Fig. 7B). In particular, the x-z axis analysis of confocal images confirms that BCRP/ABCG2 levels are elevated in the plasma membrane of A2780DR, and this was suppressed by LY294. These results show that PI3K signaling is associated with BCRP/ABCG2 overexpression in resistant cells. Next, we examined the effect of c-MET inhibitor on BCRP/ABCG2 expression. The treatment of cells with SU112 for 3-24 h decreased p-AKT levels in A2780DR, and BCPR monomer level was also repressed (Fig. 7C). This finding was also confirmed by immunocytochemical analysis: c-MET inhibitor treatment led to the reduction in plasma membrane BCRP/ABCG2 levels (Fig. 7D). To confirm the linkage between c-MET and BCRP/ABCG2, we transiently silenced c-MET expression in A2780DR using c-MET specific siRNAs (#51 and #52) and examined BCRP expression. Results indicate that the genetic inhibition of c-MET effectively reduced BCRP protein level (Fig. 7E).

c-MET-BCRP/ABCG2 signaling was confirmed in additional cancer cell lines

Our results indicate that activated c-MET signaling led to BCRP/ABCG2 overexpression and refractoriness to doxorubicin and PDT in A2780DR. Next, we questioned whether this phenomenon can be observed in additional cell lines. For this, we have selected breast carcinoma MDA-MB-231 and colon carcinoma HT29 as the c-MET overexpression cancer cell line systems, and investigated the effect of c-MET inhibition on BCRP expression and doxorubicin response. Firstly, western blot analysis showed that c-MET protein is highly expressed in these two cell lines (Fig. 8A). Secondly, when c-MET specific siRNA (#51) was transfected, BCRP protein levels were reduced in both cell lines (Fig. 8B). Accordantly, the c-MET siRNA-transfected MDA-MB-231 cells showed enhanced cell death following

Molecular Pharmacology Fast Forward. Published on December 22, 2014 as DOI: 10.1124/mol.114.096065
This article has not been copyedited and formatted. The final version may differ from this version.

doxorubicin treatment (Fig. 8C). Similarly, the SU112-treated HT29 exhibited increased doxorubicin sensitivity compared to the control cells (Fig. 8D). These results confirm that increased c-MET signaling is associated with BCRP/ABCG2 overexpression in additional cancer cells.

Discussion

In the present report, we have shown that the doxorubicin resistant ovarian carcinoma sub-cell line A2780DR overexpresses c-MET, and demonstrated that c-MET elevation led to an increased expression of drug efflux transporter BCRP/ABCG2 via PI3K/AKT signaling. Using pharmacological inhibitors and siRNA-mediated genetic inhibition, we provide evidence that elevated values of the c-MET/PI3K/BCRP axis are associated with doxorubicin resistance in A2780DR. In addition, our results indicate that c-MET-mediated chemoresistance is linked to the reduced PDT response of this cell line. Intracellular PDT accumulation, PDT-induced ROS generation, and cytotoxicity were significantly lowered in A2780DR as compared to its parental A2780 cells, whereas the inhibition of BCRP/ABCG2, PI3K/AKT or c-MET restored sensitivity to doxorubicin and PDT by repressing BCRP/ABCG2 expression. Moreover, we showed that c-MET inhibition can enhance doxorubicin sensitivity by repressing BCRP expression in additional cell lines MDA-MB-231 and HT29. Overall, these data suggest a novel link between proto-oncogene cMET and BCRP/ABCG2 activation followed by the subsequent poor response of cancer cells to doxorubicin and PDT.

PDT uses porphyrin derivatives to produce singlet oxygen and ROS through visible light irradiation, leading to apoptotic and necrotic tumor cell death (Hajri et al., 1999;

Molecular Pharmacology Fast Forward. Published on December 22, 2014 as DOI: 10.1124/mol.114.096065
This article has not been copyedited and formatted. The final version may differ from this version.

Hibasami et al., 2000; Oleinick et al., 2002; Tang et al., 2006). Pba mediates mitochondrial membrane perturbation and consequent cytochrome c release, resulting in apoptotic cell death (Tang et al., 2009). In addition, PDT destroys tumor microvasculature and causes oxygen depletion within tumors (Dougherty et al., 1998). PDT also triggers inflammation as a secondary event: the PDT-induced alteration of the plasma membrane activates acute inflammatory signaling, in turn influencing immune cell attraction to tumor tissues (Castano et al., 2006; Dougherty et al., 1998). Due to its multilateral action, PDT has been successfully applied in the clinic for the treatment of cancer of the gastrointestinal tract, lung, head, and neck in several countries, including the USA, Japan, and Europe (Dolmans et al., 2003; Dougherty et al., 1998). In the case of ovarian cancer, multiple clinical trials have been conducted showing promising results with photofrin-based PDT (Hahn et al., 2006; Hendren et al., 2001; Sindelar et al., 1991).

The development of chemoresistance has been the major hurdle in ovarian cancer treatment; the potential efficacy of PDT in chemoresistant tumors has therefore been explored. According to Casas et al. (Casas et al., 2011), about two third of current reports demonstrate the absence of cross-resistance of chemoresistant cancer cells to PDT. The *ex vivo* study using patient-derived ovarian cancer cells described that cisplatin-resistant cells can be sensitized to chemotherapy by PDT (Duska et al., 1999). In contrast, remaining reports show cross-resistance between chemotherapy and PDT; doxorubicin resistant uterine sarcoma cells displayed a reduced response to PDT (Olsen et al., 2013). Fibrosarcoma cells that are resistant to Photofrin-PDT showed low levels of cisplatin cytotoxicity and cisplatin-DNA adduct formation (Moorehead et al., 1994). These conflicting results suggest that the cellular response to PDT may be determined by multiple factors. Therefore, the potential cross-

Molecular Pharmacology Fast Forward. Published on December 22, 2014 as DOI: 10.1124/mol.114.096065
This article has not been copyedited and formatted. The final version may differ from this version.

resistance of chemoresistant ovarian cancer to PDT and its underlying molecular mechanism should be identified. In our study, ovarian cancer cells with acquired doxorubicin resistance are highly refractory to PDT cytotoxicity, supporting the development of cross-resistance to PDT.

The involvement of BCRP/ABCG2 in PDT resistance has been demonstrated in several studies. The link between photosensitizers and BCRP/ABCG2 originally emerged from a study using *bcrp*-knockout mice. Mice that are deficient in *bcrp* were more sensitive to Pba-induced skin phototoxicity (Jonker et al., 2002). It was later shown that Pba is selectively transported by BCRP/ABCG2 and treatment with BCRP/ABCG2 specific inhibitors completely blocks Pba transport (Robey et al., 2005). In addition to Pba, photofrin and photochlor, clinically approved photosensitizers, are known to be substrates of BCRP/ABCG2 (Liu et al., 2007). The above reports support the results of our study, clearly indicating that BCRP/ABCG2 expression is an important factor developing cross-resistance of ovarian cancer cells to chemotherapy and PDT. In particular, it is notable that NRF2 signaling, which is a master regulator of antioxidant gene expression, is activated in A2780DR (Shim et al., 2009); therefore, low ROS level in PDT-treated A2780DR might be caused by enhanced antioxidant proteins such as GSH synthesis enzymes. Nevertheless, the contribution of elevated BCRP/ABCG2 to PDT resistance appears to be primary. The pharmacological inhibition of BCRP/ABCG2 activity in A2780DR largely reversed Pba accumulation, ROS generation, and cell viability to the levels of A2780 (Fig. 4).

The BCRP/ABCG2 increase in cancer cells appears to be related to deviant signaling changes. In particular, there are several lines of evidence that AKT is implicated in BCRP/ABCG2 expression. The number of H342-refratory cells is decreased in *akt* null mice,

Molecular Pharmacology Fast Forward. Published on December 22, 2014 as DOI: 10.1124/mol.114.096065
This article has not been copyedited and formatted. The final version may differ from this version.

and the re-introduction of Akt in these mutant cells increased H342-negative cells, indicating that BCRP/ABCG2 activity is influenced by Akt (Mogi et al., 2003). Another group later found that AKT inhibitors reduced plasma membrane BCRP/ABCG2 expression in hepatoma cells (Hu et al., 2008). Furthermore, the activation of EGFR, an upstream regulator of PI3K/AKT, decreased BCRP overexpression cells in head and neck squamous cell carcinoma (Chen et al., 2006). These all together indicate that translocation of BCRP/ABCG2 to the plasma membrane is a critical step for BCRP activation, and this process is stimulated by PI3K/AKT signaling although specific molecular mechanisms are unveiled. Like these reports, the association of PI3K/AKT with BCRP/ABCG2 activity was verified in our A2780 system. Levels of phosphorylated AKT were higher in A2780DR than A2780, and the inhibition of PI3K/AKT reversed BCRP/ABCG2 expression and doxorubicin/PDT resistance. Further investigation showed that c-MET overexpression was related to activated PI3K/AKT signaling in A2780DR: the c-MET-specific inhibitor SU112 diminished BCRP/ABCG2 expression and doxorubicin/PDT resistance (Fig. 7). One major difference in our study is that the c-MET/PI3K/AKT axis appears to activate transcription of BCRP/ABCG2. A2780DR showed substantial increases in BCRP/ABCG2 mRNA and monomer BCRP/ABCG2 level (72 kDa), as well as its plasma membrane level (Fig. 3 and Fig. 7). In addition, treatment with an inhibitor of c-MET or PI3K/AKT reduced the level of BCRP monomer present (Fig. 7A and 7C). To our knowledge, there is no previous study describing the involvement of c-MET in BCRP/ABCG2 expression; therefore the molecular mechanism of c-MET-mediated BCRP/ABCG2 up-regulation has yet to be elucidated. One of possible mechanisms would be the up-regulation of BCRP/ABCG2 by cancer stem cell markers. There has been a report that stemness transcription factor OCT4 positively regulates BCRP/ABCG2 expression in chronic

Molecular Pharmacology Fast Forward. Published on December 22, 2014 as DOI: 10.1124/mol.114.096065
This article has not been copyedited and formatted. The final version may differ from this version.

myeloid leukemia (Marques et al., 2010). Furthermore, lines of evidence showed that c-MET is involved in the maintenance of cancer stem cell phenotypes (Boccaccio and Comoglio, 2013). These suggest that the increase in c-MET-mediated stemness makers may be associated with BCRP overexpression. In addition, since we previously observed that NRF2 signaling is enhanced in A2780DR (Shim et al., 2009), there is a possibility that elevated BCRP/ABCG2 expression is partly attributable to NRF2 activation. However, given that NRF2 regulates the expression of multiple transporters including MRP/ABCC and MDR1/ABCB1 (Adachi et al., 2007; Hayashi et al., 2003; Maher et al., 2005), the exclusive increase of BCRP/ABCG2 in this case is still mysterious.

Aberrant activation of c-MET is strongly linked to increased tumorigenecity and metastasis potential in various types of cancer. In advanced ovarian carcinoma, high levels of c-MET expression were correlated with poor survival rates (Ayhan et al., 2005; Wong et al., 2001). Similarly, c-MET activation was related to increased expression of migration-associated genes such as MMP-2 and MMP-9 in ovarian cancer (Sawada et al., 2007). Therefore, blockage of c-MET signaling using pharmacological inhibitors may suppress cell growth, motility and invasion in ovarian carcinoma cell lines (Koon et al., 2008). In addition to these phenotypic characteristics, c-MET was implicated in the chemoresistance of cancer cells. The incubation of gastric carcinoma cells with the c-MET inhibitor SU112 sensitized cells to irinotecan (Yashiro et al., 2013). c-MET was overexpressed in a chemoresistant multiple myeloma cell line; SU112 treatment countered this cell line's resistance to melphalan, bortezomib, and doxorubicin (Moschetta et al., 2013). Ovarian cancer patients with higher levels of relapse after chemotherapy showed elevated expression of c-MET and HGF (Mariani et al., 2014). Our study supports the above reports in that it provides evidence

that doxorubicin resistance is attributed to an increase of c-MET levels in ovarian carcinoma cells. In addition, we present up-regulation of BCRP/ABCG2 as a novel mechanism of c-MET chemoresistance in ovarian, breast and colon carcinoma cells, although the genetic variations in these cell lines are divergent. Several factors have been suggested to be involved in the overexpression of c-MET. Particularly, the *c-MET* promoter analysis revealed that ETS1 directly activates c-MET transcription (Gambarotta et al., 1996). The ETS1 increase elevated c-MET expression and consequently enhanced expression of genes involved in malignant phenotypes (Furlan et al., 2008). Whereas, in A2780DR, ETS1 is not likely to induce an increase in c-MET expression: ETS-1 levels were not different from those in A2780 in our microarray analysis (data not shown). On the other hand, since wild-type p53 was reported to repress c-MET expression through changes in miR-34a (Hwang et al., 2011), a reasonable hypothesis is that continuous doxorubicin exposure evokes mutation of p53, resulting in c-MET overexpression.

In conclusion, our present study shows that c-MET overexpression is accompanied by the acquisition of adaptive resistance to doxorubicin in A2780, suggesting that the consequent activation of c-MET/PI3K/AKT signaling elicits elevation of BCRP/ABCG2 levels, leading to resistance to both chemotherapy and PDT in cancer cells.

Molecular Pharmacology Fast Forward. Published on December 22, 2014 as DOI: 10.1124/mol.114.096065
This article has not been copyedited and formatted. The final version may differ from this version.

Acknowledgements: The authors thank Dr. Han Chang Kang from The Catholic University of Korea for allowing the access to some facilities and for his helpful discussion.

Authors' contributions:

Participated in research design: M-K Kwak

Conducted experiments: K-A Jung, B-H Choi

Contributed new reagents or analytic tools: K-A Jung, B-H Choi, M-K Kwak

Performed data analysis: K-A Jung, B-H Choi, M-K Kwak

Wrote or contributed to the writing of the manuscript: M-K Kwak, K-A Jung, B-H Choi

K-A Jung and B-H Choi contributed equally to this work.

Disclosure of potential conflicts of interest: No potential conflicts of interest were disclosed.

References

Adachi T, Nakagawa H, Chung I, Hagiya Y, Hoshijima K, Noguchi N, Kuo MT and Ishikawa T (2007) Nrf2-dependent and -independent induction of ABC transporters ABCC1, ABCC2, and ABCG2 in HepG2 cells under oxidative stress. *Journal of experimental therapeutics & oncology* **6**(4): 335-348.

An Y and Ongkeko WM (2009) ABCG2: the key to chemoresistance in cancer stem cells? *Expert opinion on drug metabolism & toxicology* **5**(12): 1529-1542.

Ayhan A, Ertunc D, Tok EC and Ayhan A (2005) Expression of the c-Met in advanced epithelial ovarian cancer and its prognostic significance. *International journal of gynecological cancer* **15**(4): 618-623.

Boccaccio C and Comoglio PM (2013) The MET oncogene in glioblastoma stem cells: implications as a diagnostic marker and a therapeutic target. *Cancer research* **73**(11): 3193-3199.

Buytaert E, Dewaele M and Agostinis P (2007) Molecular effectors of multiple cell death pathways initiated by photodynamic therapy. *Biochimica et biophysica acta* **1776**(1): 86-107.

Casas A, Di Venosa G, Hasan T and Al B (2011) Mechanisms of resistance to photodynamic therapy. *Current medicinal chemistry* **18**(16): 2486-2515.

Castano AP, Mroz P and Hamblin MR (2006) Photodynamic therapy and anti-tumour immunity. *Nature reviews Cancer* **6**(7): 535-545.

Chan JY, Tang PM, Hon PM, Au SW, Tsui SK, Waye MM, Kong SK, Mak TC and Fung KP (2006) Pheophorbide a, a major antitumor component purified from Scutellaria barbata, induces apoptosis in human hepatocellular carcinoma cells. *Planta medica* **72**(1): 28-33.

Chen JS, Pardo FS, Wang-Rodriguez J, Chu TS, Lopez JP, Aguilera J, Altuna X, Weisman RA and Ongkeko WM (2006) EGFR regulates the side population in head and neck squamous cell carcinoma. *The Laryngoscope* **116**(3): 401-406.

Choi BH, Ryoo IG, Kang HC and Kwak MK (2014) The sensitivity of cancer cells to pheophorbide a-based photodynamic therapy is enhanced by Nrf2 silencing. *PloS one* **9**(9): e107158.

Dolmans DE, Fukumura D and Jain RK (2003) Photodynamic therapy for cancer. *Nature*

reviews Cancer **3**(5): 380-387.

Dougherty TJ, Gomer CJ, Henderson BW, Jori G, Kessel D, Korbelik M, Moan J and Peng Q (1998) Photodynamic therapy. *Journal of the National Cancer Institute* **90**(12): 889-905.

Doyle LA, Yang W, Abruzzo LV, Krogmann T, Gao Y, Rishi AK and Ross DD (1998) A multidrug resistance transporter from human MCF-7 breast cancer cells. *Proceedings of the National Academy of Sciences of the United States of America* **95**(26): 15665-15670.

Duska LR, Hamblin MR, Miller JL and Hasan T (1999) Combination photoimmunotherapy and cisplatin: effects on human ovarian cancer ex vivo. *Journal of the National Cancer Institute* **91**(18): 1557-1563.

Furlan A, Vercamer C, Desbiens X and Pourtier A (2008) Ets-1 triggers and orchestrates the malignant phenotype of mammary cancer cells within their matrix environment. *Journal of cellular physiology* **215**(3): 782-793.

Gambarotta G, Boccaccio C, Giordano S, Ando M, Stella MC and Comoglio PM (1996) Ets up-regulates MET transcription. *Oncogene* **13**(9): 1911-1917.

Ghiso E and Giordano S (2013) Targeting MET: why, where and how? *Current opinion in pharmacology* **13**(4): 511-518.

Graveel CR, Tolbert D and Vande Woude GF (2013) MET: a critical player in tumorigenesis and therapeutic target. *Cold Spring Harbor perspectives in biology* **5**(7): a009209.

Hahn SM, Fraker DL, Mick R, Metz J, Busch TM, Smith D, Zhu T, Rodriguez C, Dimofte A, Spitz F, Putt M, Rubin SC, Menon C, Wang HW, Shin D, Yodh A and Glatstein E (2006) A phase II trial of intraperitoneal photodynamic therapy for patients with peritoneal carcinomatosis and sarcomatosis. *Clinical cancer research* **12**(8): 2517-2525.

Hajri A, Coffy S, Vallat F, Evrard S, Marescaux J and Aprahamian M (1999) Human pancreatic carcinoma cells are sensitive to photodynamic therapy in vitro and in vivo. *The British journal of surgery* **86**(7): 899-906.

Hajri A, Wack S, Meyer C, Smith MK, Leberquier C, Kedinger M and Aprahamian M (2002) In vitro and in vivo efficacy of photofrin and pheophorbide a, a bacteriochlorin, in photodynamic therapy of colonic cancer cells. *Photochemistry and photobiology*

75(2): 140-148.

Hayashi A, Suzuki H, Itoh K, Yamamoto M and Sugiyama Y (2003) Transcription factor Nrf2 is required for the constitutive and inducible expression of multidrug resistance-associated protein 1 in mouse embryo fibroblasts. *Biochemical and biophysical research communications* **310**(3): 824-829.

Hendren SK, Hahn SM, Spitz FR, Bauer TW, Rubin SC, Zhu T, Glatstein E and Fraker DL (2001) Phase II trial of debulking surgery and photodynamic therapy for disseminated intraperitoneal tumors. *Annals of surgical oncology* **8**(1): 65-71.

Hibasami H, Kyohkon M, Ohwaki S, Katsuzaki H, Imai K, Nakagawa M, Ishi Y and Komiya T (2000) Pheophorbide a, a moiety of chlorophyll a, induces apoptosis in human lymphoid leukemia molt 4B cells. *International journal of molecular medicine* **6**(3): 277-279.

Hopper C (2000) Photodynamic therapy: a clinical reality in the treatment of cancer. *The lancet oncology* **1**: 212-219.

Hu C, Li H, Li J, Zhu Z, Yin S, Hao X, Yao M, Zheng S and Gu J (2008) Analysis of ABCG2 expression and side population identifies intrinsic drug efflux in the HCC cell line MHCC-97L and its modulation by Akt signaling. *Carcinogenesis* **29**(12): 2289-2297.

Humphrey PA, Zhu X, Zarnegar R, Swanson PE, Ratliff TL, Vollmer RT and Day ML (1995) Hepatocyte growth factor and its receptor (c-MET) in prostatic carcinoma. *The American journal of pathology* **147**(2): 386-396.

Hwang CI, Matoso A, Corney DC, Flesken-Nikitin A, Korner S, Wang W, Boccaccio C, Thorgeirsson SS, Comoglio PM, Hermeking H and Nikitin AY (2011) Wild-type p53 controls cell motility and invasion by dual regulation of MET expression. *Proceedings of the National Academy of Sciences of the United States of America* **108**(34): 14240-14245.

Ichimura E, Maeshima A, Nakajima T and Nakamura T (1996) Expression of c-met/HGF receptor in human non-small cell lung carcinomas in vitro and in vivo and its prognostic significance. *Japanese journal of cancer research : Gann* **87**(10): 1063-1069.

Jamieson D and Boddy AV (2011) Pharmacogenetics of genes across the doxorubicin pathway. *Expert opinion on drug metabolism & toxicology* **7**(10): 1201-1210.

Jonker JW, Buitelaar M, Wagenaar E, Van Der Valk MA, Scheffer GL, Scheper RJ, Plosch T, Kuipers F, Elferink RP, Rosing H, Beijnen JH and Schinkel AH (2002) The breast cancer resistance protein protects against a major chlorophyll-derived dietary phototoxin and protoporphyria. *Proceedings of the National Academy of Sciences of the United States of America* **99**(24): 15649-15654.

Koon EC, Ma PC, Salgia R, Welch WR, Christensen JG, Berkowitz RS and Mok SC (2008) Effect of a c-Met-specific, ATP-competitive small-molecule inhibitor SU11274 on human ovarian carcinoma cell growth, motility, and invasion. *International journal of gynecological cancer* **18**(5): 976-984.

Krishnamurthy P, Ross DD, Nakanishi T, Bailey-Dell K, Zhou S, Mercer KE, Sarkadi B, Sorrentino BP and Schuetz JD (2004) The stem cell marker Bcrp/ABCG2 enhances hypoxic cell survival through interactions with heme. *The Journal of biological chemistry* **279**(23): 24218-24225.

Li WT, Tsao HW, Chen YY, Cheng SW and Hsu YC (2007) A study on the photodynamic properties of chlorophyll derivatives using human hepatocellular carcinoma cells. *Photochemical & photobiological sciences* **6**(12): 1341-1348.

Litman T, Brangi M, Hudson E, Fetsch P, Abati A, Ross DD, Miyake K, Resau JH and Bates SE (2000) The multidrug-resistant phenotype associated with overexpression of the new ABC half-transporter, MXR (ABCG2). *Journal of cell science* **113 (Pt 11)**: 2011-2021.

Liu W, Baer MR, Bowman MJ, Pera P, Zheng X, Morgan J, Pandey RA and Oseroff AR (2007) The tyrosine kinase inhibitor imatinib mesylate enhances the efficacy of photodynamic therapy by inhibiting ABCG2. *Clinical cancer research* **13**(8): 2463-2470.

Maher JM, Cheng X, Slitt AL, Dieter MZ and Klaassen CD (2005) Induction of the multidrug resistance-associated protein family of transporters by chemical activators of receptor-mediated pathways in mouse liver. *Drug metabolism and disposition: the biological fate of chemicals* **33**(7): 956-962.

Mariani M, McHugh M, Petrillo M, Sieber S, He S, Andreoli M, Wu Z, Fiedler P, Scambia G, Shahabi S and Ferlini C (2014) HGF/c-Met axis drives cancer aggressiveness in the neo-adjuvant setting of ovarian cancer. *Oncotarget* **5**(13): 4855-4867.

Marques DS, Sandrini JZ, Boyle RT, Marins LF and Trindade GS (2010) Relationships between multidrug resistance (MDR) and stem cell markers in human chronic myeloid leukemia cell lines. *Leukemia research* **34**(6): 757-762.

Minotti G, Menna P, Salvatorelli E, Cairo G and Gianni L (2004) Anthracyclines: molecular advances and pharmacologic developments in antitumor activity and cardiotoxicity. *Pharmacological Reiew* **56**(2): 185-229.

Mogi M, Yang J, Lambert JF, Colvin GA, Shiojima I, Skurk C, Summer R, Fine A, Quesenberry PJ and Walsh K (2003) Akt signaling regulates side population cell phenotype via Bcrp1 translocation. *The Journal of biological chemistry* **278**(40): 39068-39075.

Moorehead RA, Armstrong SG, Wilson BC and Singh G (1994) Cross-resistance to cisplatin in cells resistant to photofrin-mediated photodynamic therapy. *Cancer research* **54**(10): 2556-2559.

Moschetta M, Basile A, Ferrucci A, Frassanito MA, Rao L, Ria R, Solimando AG, Giuliani N, Boccarelli A, Fumarola F, Coluccia M, Rossini B, Ruggieri S, Nico B, Maiorano E, Ribatti D, Roccaro AM and Vacca A (2013) Novel targeting of phospho-cMET overcomes drug resistance and induces antitumor activity in multiple myeloma. *Clinical cancer research* **19**(16): 4371-4382.

Muller I, Niethammer D and Bruchelt G (1998) Anthracycline-derived chemotherapeutics in apoptosis and free radical cytotoxicity (Review). *International journal of molecular medicine* **1**(2): 491-494.

Oleinick NL, Morris RL and Belichenko I (2002) The role of apoptosis in response to photodynamic therapy: what, where, why, and how. *Photochemical & photobiological sciences* **1**(1): 1-21.

Olsen CE, Berg K, Selbo PK and Weyergang A (2013) Circumvention of resistance to photodynamic therapy in doxorubicin-resistant sarcoma by photochemical internalization of gelonin. *Free radical biology & medicine* **65**: 1300-1309.

Park YJ, Lee WY, Hahn BS, Han MJ, Yang WI and Kim BS (1989) Chlorophyll derivatives--a new photosensitizer for photodynamic therapy of cancer in mice. *Yonsei medical journal* **30**(3): 212-218.

Robey RW, Steadman K, Polgar O and Bates SE (2005) ABCG2-mediated transport of

photosensitizers: potential impact on photodynamic therapy. *Cancer biology & therapy* **4**(2): 187-194.

Sawada K, Radjabi AR, Shinomiya N, Kistner E, Kenny H, Becker AR, Turkyilmaz MA, Salgia R, Yamada SD, Vande Woude GF, Tretiakova MS and Lengyel E (2007) c-Met overexpression is a prognostic factor in ovarian cancer and an effective target for inhibition of peritoneal dissemination and invasion. *Cancer research* **67**(4): 1670-1679.

Sharman WM, Allen CM and van Lier JE (2000) Role of activated oxygen species in photodynamic therapy. *Methods in enzymology* **319**: 376-400.

Shim GS, Manandhar S, Shin DH, Kim TH and Kwak MK (2009) Acquisition of doxorubicin resistance in ovarian carcinoma cells accompanies activation of the NRF2 pathway. *Free radical biology & medicine* **47**(11): 1619-1631.

Sindelar WF, DeLaney TF, Tochner Z, Thomas GF, Dachoswki LJ, Smith PD, Friauf WS, Cole JW and Glatstein E (1991) Technique of photodynamic therapy for disseminated intraperitoneal malignant neoplasms. Phase I study. *Archives of surgery (Chicago, Ill : 1960)* **126**(3): 318-324.

Singh G, Espiritu M, Shen XY, Hanlon JG and Rainbow AJ (2001) In vitro induction of PDT resistance in HT29, HT1376 and SK-N-MC cells by various photosensitizers. *Photochemistry and photobiology* **73**(6): 651-656.

Stacy AE, Jansson PJ and Richardson DR (2013) Molecular pharmacology of ABCG2 and its role in chemoresistance. *Molecular pharmacology* **84**(5): 655-669.

Szatmari I, Vamosi G, Brazda P, Balint BL, Benko S, Szeles L, Jeney V, Ozvegy-Laczka C, Szanto A, Barta E, Balla J, Sarkadi B and Nagy L (2006) Peroxisome proliferator-activated receptor gamma-regulated ABCG2 expression confers cytoprotection to human dendritic cells. *The Journal of biological chemistry* **281**(33): 23812-23823.

Tang PM, Chan JY, Au SW, Kong SK, Tsui SK, Waye MM, Mak TC, Fong WP and Fung KP (2006) Pheophorbide a, an active compound isolated from Scutellaria barbata, possesses photodynamic activities by inducing apoptosis in human hepatocellular carcinoma. *Cancer biology & therapy* **5**(9): 1111-1116.

Tang PM, Liu XZ, Zhang DM, Fong WP and Fung KP (2009) Pheophorbide a based photodynamic therapy induces apoptosis via mitochondrial-mediated pathway in

human uterine carcinosarcoma. *Cancer biology & therapy* **8**(6): 533-539.

Wang H, Zhou L, Gupta A, Vethanayagam RR, Zhang Y, Unadkat JD and Mao Q (2006) Regulation of BCRP/ABCG2 expression by progesterone and 17beta-estradiol in human placental BeWo cells. *American journal of physiology Endocrinology and metabolism* **290**(5): E798-807.

Wong AS, Pelech SL, Woo MM, Yim G, Rosen B, Ehlen T, Leung PC and Auersperg N (2001) Coexpression of hepatocyte growth factor-Met: an early step in ovarian carcinogenesis? *Oncogene* **20**(11): 1318-1328.

Xodo LE, Rapozzi V, Zacchigna M, Drioli S and Zorzet S (2012) The chlorophyll catabolite pheophorbide a as a photosensitizer for the photodynamic therapy. *Current medicinal chemistry* **19**(6): 799-807.

Yashiro M, Nishii T, Hasegawa T, Matsuzaki T, Morisaki T, Fukuoka T and Hirakawa K (2013) A c-Met inhibitor increases the chemosensitivity of cancer stem cells to the irinotecan in gastric carcinoma. *British journal of cancer* **109**(10): 2619-2628.

Molecular Pharmacology Fast Forward. Published on December 22, 2014 as DOI: 10.1124/mol.114.096065
This article has not been copyedited and formatted. The final version may differ from this version.

Footnotes

This study was financially supported by the National Research Foundation (NRF) funded by the Ministry of Science, ICT & Future Planning [NRF-2013R1A2A2A01015497].

Molecular Pharmacology Fast Forward. Published on December 22, 2014 as DOI: 10.1124/mol.114.096065
This article has not been copyedited and formatted. The final version may differ from this version.

Legends for figures

Figure 1. A2780DR is resistant to doxorubicin accumulation and PDT cytotoxicity. (A) A2780 and A2780DR were treated with doxorubicin (0 – 1.6 μM) for 48 h and MTT analysis was performed. The data represent ratios with respect to the vehicle group for each cell line and are reported as the mean ± standard error (SE) of 8 wells. $^{a}P < 0.05$ as compared with A2780. (B) The cells were incubated with doxorubicin (0 – 4 μM) for 6 h followed by PBS washing and fluorogenic doxorubicin was visualized using a Cell Insight system. Relative levels of cellular doxorubicin in A2780 and A2780DR were quantified. The data are ratios with respect to the vehicle control and are reported as the mean ± SE of 3-4 experiments. $^{a}P < 0.05$ as compared with A2780. (C) A2780 and A2780DR were incubated with Pba (0 – 0.25 μg/ml) for 24 h and viable cell numbers were assessed using MTT analysis. (D) The cells were incubated with Pba for 6 h and then were irradiated by laser light (0.3 J/cm^2). Cells were recovered in a complete medium for 18 h and MTT analysis was carried out. The data are percentages with respect to the Pba only group and are reported as the mean ± SE of 8-10 wells. $^{a}P < 0.05$ as compared with A2780.

Figure 2. Levels of singlet oxygen, ROS, and Pba cellular accumulation are low in A2780DR. (A) The cells were incubated with Pba for 6 h and were irradiated by laser light. Right after PDT, a singlet oxygen sensitive trans-1-(2'-methoxyvinyl) pyrene was added and cells were further incubated for 30 min. A confocal observation was performed to detect singlet oxygen-derived fluorogenic pyrene formation (x1,000 magnification). Green fluorescence intensity was quantified with ZEN 2011 software. (B) After PDT, A2780 and A2780DR were incubated with DCFDA for 30 min, and ROS-derived green fluorescence was detected with

Molecular Pharmacology Fast Forward. Published on December 22, 2014 as DOI: 10.1124/mol.114.096065
This article has not been copyedited and formatted. The final version may differ from this version.

confocal microscope (x1,000 magnification). The data represent ratios with respect to the no PDT control and are reported as the mean ± SE of 3-4 experiments. $^{a}P < 0.05$ as compared with A2780 of each concentration of Pba. (C) The cells were incubated with Pba (2.5 μg/ml) for 6 h and then washed with PBS. Intracellular accumulation of Pba was monitored by detecting red fluorescence using a confocal microscopy (x1,000 magnification). A bar graph represents relative cellular levels of Pba with respect to the no Pba control and are reported as the mean ± SE of 3-4 experiments. $^{a}P < 0.05$ as compared with A2780.

Figure 3. Elevated BCRP/ABCG2 expression in A2780DR is associated with doxorubicin resistance. (A) Transcript levels for BCRP/ABCG2, MDR1/ABCB1 and MRP1-2/ABCC1-2 were determined in A2780 and A2780DR using a relative quantification of RT-PCR analysis. The data represent ratios with respect to A2780 of each gene and are reported as the mean ± SE of 3-4 experiments. (B) Protein levels of BCRP/ABCG2 were determined using western blot analysis. Similar blots were obtained from 3-4 independent experiments. (C) An immunocytochemcial detection of BCRP/ABCG2 was performed using a confocal microscopic observation. Nuclei were stained with PI. x1,000 magnification (D) A2780 and A2780DR were incubated with BCRP/ABCG2 substrate H342 for 10 min and cellular level of H342 fluorescence intensities were quantified. The data represent ratios with respect to A2780 and are reported as the mean ± SE of 3-4 experiments. (E) Cells were incubated with MRP substrate CMF-DA (1 and 2 μM) for 10 min, PBS washing followed and cellular fluorescent intensities were quantified. The data represent ratios with respect to vehicle control of each cell line and are reported as the mean ± SE of 3-4 experiments. (F) A2780 and A2780DR were pre-incubated with BCRP/ABCG2 specific inhibitor Ko143 (0.5 and 1 μM)

for 1 h and then vehicle or doxorubicin (2 μM) was added for a further 6 h-incubation. Intracellular levels of doxorubicin were quantified using a Cell Insight system. The data are ratios with respect to the A2780 vehicle control and are reported as the mean ± SE of 8-10 wells. [a]$P < 0.05$ as compared with the A2780 doxorubicin alone group. [b]$P < 0.05$ as compared with A2780DR doxorubicin alone group.

Figure 4. A2780DR shows a lower level of cellular Pba accumulation via elevated BCRP/ABCG2 expression. (A) A2780 and A2780DR were pre-incubated with Ko143 (1 μM) for 1 h and then Pba (0.25 and 2.5 μg/ml) was added for a further 6 h-incubation. Cellular level of Pba was visualized using a confocal microscopic observation. Pba-derived red fluorescent intensities were quantified using a Cell Insight system (bar graph). The data are ratios with respect to the A2780 vehicle control and are reported as the mean ± SE of 3-4 experiments. (B) Levels of singlet oxygen were assessed in cells treated with Pba-PDT in the presence or absence of Ko143 (1 μM). Green fluorescence intesities from singlet oxygen reacted dye were quantified using a Cell Insight system. The data are average fluorescence intensities and are reported as the mean ± SE of 3-4 experiments. (C) Viable cell numbers were monitored in PDT-cells with or without Ko143 incubation (1 μM). Cells were incubated with Pba (0.25 μg/ml) for 6 h and MTT analysis was performed at 24 h after PDT. The data are percentages with respect to the no PDT group of each cell line and are reported as the mean ± SE of 8-10 wells. [a]$P < 0.05$ as compared with the A2780 vehicle group. [b]$P < 0.05$ as compared with A2780DR vehicle group.

Molecular Pharmacology Fast Forward. Published on December 22, 2014 as DOI: 10.1124/mol.114.096065
This article has not been copyedited and formatted. The final version may differ from this version.

Figure 5. Enhanced c-MET expression in A2780DR is involved in reduced doxorubicin accumulation. (A) Relative transcript levels of c-MET and HGF were measured in A2780 and A2780DR using a real time RT-PCR analysis. The data are ratios with respect to the A2780 group of each gene and are reported as the mean ± SE of 3 experiments. $^{a}P < 0.05$ as compared with A2780. (B) Protein levels for c-MET, p85 subunit of PI3K, and phosphorylated (Ser473) and total AKT were determined in A2780 and A2780DR. (C-D) Cellular accumulation level of doxorubicin was monitored following the incubation with PI3K inhibitor (LY294; 5 and 10 μM) or c-MET inhibitor (SU112; 1 and 2 μM). A2780 and A2780DR were incubated with doxorubicin (2 μM) for 6 h in the presence or absence of LY 294 (C) or SU112 (D), PBS washing followed and cellular fluorescent intensities were quantified using a Cell Insight system. The data are ratios with respect to the vehicle control of each cell line and are reported as the mean ± SE of 3 experiments. $^{a}P < 0.05$ as compared with the A2780 doxorubicin alone group. $^{b}P < 0.05$ as compared with the A2780DR doxorubicin alone group. (E) Viable cell numbers were estimated in doxorubicin-treated cells in the presence of SU112. The data are ratios with respect to vehicle control of each cell line and are reported as the mean ± SE of 3 experiments. $^{a}P < 0.05$ as compared with the A2780DR doxorubicin alone group.

Figure 6. Pba accumulation, singlet oxygen generation and PDT cytotoxicity are repressed by the inhibition of PI3K/AKT or c-MET. (A) Cellular accumulation level of Pba was assessed following PI3K inhibitor treatment. LY294 (5 μM) was pre-incubated for 3 h and then Pba was followed for a further 6 h-incubation. A confocal microscopic observation was performed (x1,000 magnification). (B) Cellular level of singlet oxygen was determined in

Molecular Pharmacology Fast Forward. Published on December 22, 2014 as DOI: 10.1124/mol.114.096065
This article has not been copyedited and formatted. The final version may differ from this version.

cells with PDT in the presence or absence of PI3K inhibitor. PDT (0.25 and 2.5 μg/ml Pba) was performed in the LY294-pretreated cells, and then trans-1-(2′methoxyvinyl) pyrene was incubated for 30 min. Green fluorescence from singlet oxygen-reacted dye was quantified using a Cell Insight system. The data are average fluorescent intensities and are reported as the mean ± SE of 3-4 experiments. $^{a}P < 0.05$ as compared with the A2780DR PDT only group. (C) Effect of LY294 on PDT-cell viability was evaluated. PDT was performed in LY294-pretreated cells and viable cell number was determined after 24 h using a MTT analysis. The data are percentages with respect to the no PDT group of each cell line and are reported as the mean ± SE of 8-10 wells. $^{a}P < 0.05$ as compared with the A2780 vehicle group. $^{b}P < 0.05$ as compared with A2780DR vehicle group. (D) Cellular accumulation level of Pba was assessed following c-MET inhibitor incubation. Pba incubation (6 h) was carried out in SU112 (1 μM)-pretreated cells and then a confocal microscopic observation was performed (x1,000 magnification). (E) Cellular level of singlet oxygen was determined in cells with PDT in the presence or absence of c-MET inhibitor. Cells were pre-incubated with SU112 and PDT (0.25 and 2.5 μg/ml Pba) was followed. $^{a}P < 0.05$ as compared with the A2780DR PDT only group. (F) PDT was performed in SU112-pretreated cells and viable cell numbers were determined after 24 h using a MTT analysis. The data are percentages with respect to the no PDT group of each cell line and are reported as the mean ± SE of 8-10 wells. $^{a}P < 0.05$ as compared with the A2780 vehicle group. $^{b}P < 0.05$ as compared with A2780DR vehicle group.

Figure 7. The inhibition of PI3K/AKT or c-MET suppresses BCRP/ABCG2 expression in A2780DR. (A) Protein levels for p-AKT and BCRP/ABCG2 were examined in LY294 (5 μM, 3-24 h)-treated cells using a western blot analysis. (B) An immunocytochemical observation

Molecular Pharmacology Fast Forward. Published on December 22, 2014 as DOI: 10.1124/mol.114.096065
This article has not been copyedited and formatted. The final version may differ from this version.

of BCRP/ABCG2 was carried out using a confocal microscopy (x1,000 magnification). A2780 and A2780DR were incubated with LY294 for 3, 24 h and BCRP/ABCG2 expression was visualized. The x-z axis images show that the level of plasma membrane BCRP/ABCG2 was altered by LY294. (C) Protein levels for c-MET, p85 subunit of PI3K, p-AKT and BCRP/ABCG2 were examined in cells treated with SU112 compound (1 μM, 3-24 h). (D) BCRP/ABCG2 expression was visualized using an immunocytochemical analysis (x1,000 magnification). The x-z axis images confirm the alteration of plasma membrane BCRP/ABCG2 by SU112. In all experimental demonstrations, similar results were obtained from 3-4 independent experiments. (E) A2780DR was transiently transfected with c-MET specific siRNA (#51 and #52), and mRNA level of c-MET and protein level of BCRP were assessed. Similar blots were obtained from 2-3 experiments.

Figure 8. c-MET inhibition represses BCRP level in breast and colon carcinoma cell lines. (A) c-MET protein levels were determined in MDA-MB-231 and HT29 using western blot analysis. (B) MDA-MB-231 and HT29 were transfected with c-MET siRNA, and then mRNA levels for c-MET and protein levels for BCRP were assessed. (C) MDA-MB-231 was transfected with c-MET siRNA, and doxorubicin cytotoxicity was monitored. Doxorubicin was incubated for 48 h, and MTT analysis was performed. (D) HT29 was pre-incubated with SU112, and doxorubicin cytotoxicity was examined using MTT analysis. The data represent ratios with respect to the vehicle group and are reported as the mean ± standard error (SE) of 8 wells. $^{a}P < 0.05$ as compared with sc or doxorubicin alone group.

Molecular Pharmacology Fast Forward. Published on December 22, 2014 as DOI: 10.1124/mol.114.096065
This article has not been copyedited and formatted. The final version may differ from this version.

Table 1. Differentially expressed ABC transporters in A2780DR

Description	Gene name	Fold change (A2780DR/A2780)
ATP-binding cassette, sub-family A (ABC1), member 1	ABCA1	0.446
ATP-binding cassette, sub-family A (ABC1), member 2	ABCA2	1.108
ATP-binding cassette, sub-family A (ABC1), member 3	ABCA3	1.270
ATP-binding cassette, sub-family A (ABC1), member 4	ABCA4	0.931
ATP-binding cassette, sub-family A (ABC1), member 5	ABCA5	0.500
ATP-binding cassette, sub-family A (ABC1), member 6	ABCA6	0.908
ATP-binding cassette, sub-family A (ABC1), member 7	ABCA7	1.012
ATP-binding cassette, sub-family A (ABC1), member 8	ABCA8	1.000
ATP-binding cassette, sub-family A (ABC1), member 9	ABCA9	1.234
ATP-binding cassette, sub-family A (ABC1), member 10	ABCA10	0.917
ATP-binding cassette, sub-family A (ABC1), member 11	ABCA11	0.885
ATP-binding cassette, sub-family A (ABC1), member 12	ABCA12	0.972
ATP-binding cassette, sub-family A (ABC1), member 13	ABCA13	1.000
ATP-binding cassette, sub-family B (MDR/TAP), member 1	ABCB1	1.003
ATP-binding cassette, sub-family B (MDR/TAP), member 4	ABCB4	1.133
ATP-binding cassette, sub-family B (MDR/TAP), member 5	ABCB5	0.465
ATP-binding cassette, sub-family B (MDR/TAP), member 6	ABCB6	0.959
ATP-binding cassette, sub-family B (MDR/TAP), member 7	ABCB7	0.994
ATP-binding cassette, sub-family B (MDR/TAP), member 8	ABCB8	1.184
ATP-binding cassette, sub-family B (MDR/TAP), member 9	ABCB9	1.213
ATP-binding cassette, sub-family B (MDR/TAP), member 10	ABCB10	0.817
ATP-binding cassette, sub-family B (MDR/TAP), Transpoter1	TAP1	0.211
ATP-binding cassette, sub-family B (MDR/TAP), Transpoter2	TAP2	0.501
ATP-binding cassette, sub-family C (CFTR/MRP), member 1	ABCC1	0.990
ATP-binding cassette, sub-family C (CFTR/MRP), member 2	ABCC2	1.133
ATP-binding cassette, sub-family C (CFTR/MRP), member 3	ABCC3	1.008
ATP-binding cassette, sub-family C (CFTR/MRP), member 4	ABCC4	0.875
ATP-binding cassette, sub-family C (CFTR/MRP), member 5	ABCC5	0.960
ATP-binding cassette, sub-family C (CFTR/MRP), member 6	ABCC6	1.000
ATP-binding cassette, sub-family C (CFTR/MRP), member 7	ABCC7	0.886
ATP-binding cassette, sub-family C (CFTR/MRP), member 8	ABCC8	1.144
ATP-binding cassette, sub-family C (CFTR/MRP), member 9	ABCC9	0.959
ATP-binding cassette, sub-family C (CFTR/MRP), member 10	ABCC10	1.025
ATP-binding cassette, sub-family C (CFTR/MRP), member 11	ABCC11	0.813

Molecular Pharmacology Fast Forward. Published on December 22, 2014 as DOI: 10.1124/mol.114.096065
This article has not been copyedited and formatted. The final version may differ from this version.

Table 1. Continued

ATP-binding cassette, sub-family C (CFTR/MRP), member 12	ABCC12	0.491
ATP-binding cassette, sub-family C (CFTR/MRP), member 13	ABCC13	0.943
ATP-binding cassette, sub-family D (ALD), member 1	ABCD1	0.926
ATP-binding cassette, sub-family D (ALD), member 2	ABCD2	1.281
ATP-binding cassette, sub-family D (ALD), member 3	ABCD3	1.219
ATP-binding cassette, sub-family D (ALD), member 4	ABCD4	1.096
ATP-binding cassette, sub-family E (OABP), member 1	ABCE1	0.797
ATP-binding cassette, sub-family F (GCN20), member 1	ABCF1	0.928
ATP-binding cassette, sub-family F (GCN20), member 2	ABCF2	0.899
ATP-binding cassette, sub-family F (GCN20), member 3	ABCF3	1.003
ATP-binding cassette, sub-family G (WHITE), member 1	ABCG1	1.376
ATP-binding cassette, sub-family G (WHITE), member 2	**ABCG2**	**44.714**
ATP-binding cassette, sub-family G (WHITE), member 4	ABCG4	0.861
ATP-binding cassette, sub-family G (WHITE), member 5	ABCG5	0.756
ATP-binding cassette, sub-family G (WHITE), member 8	ABCG8	0.923

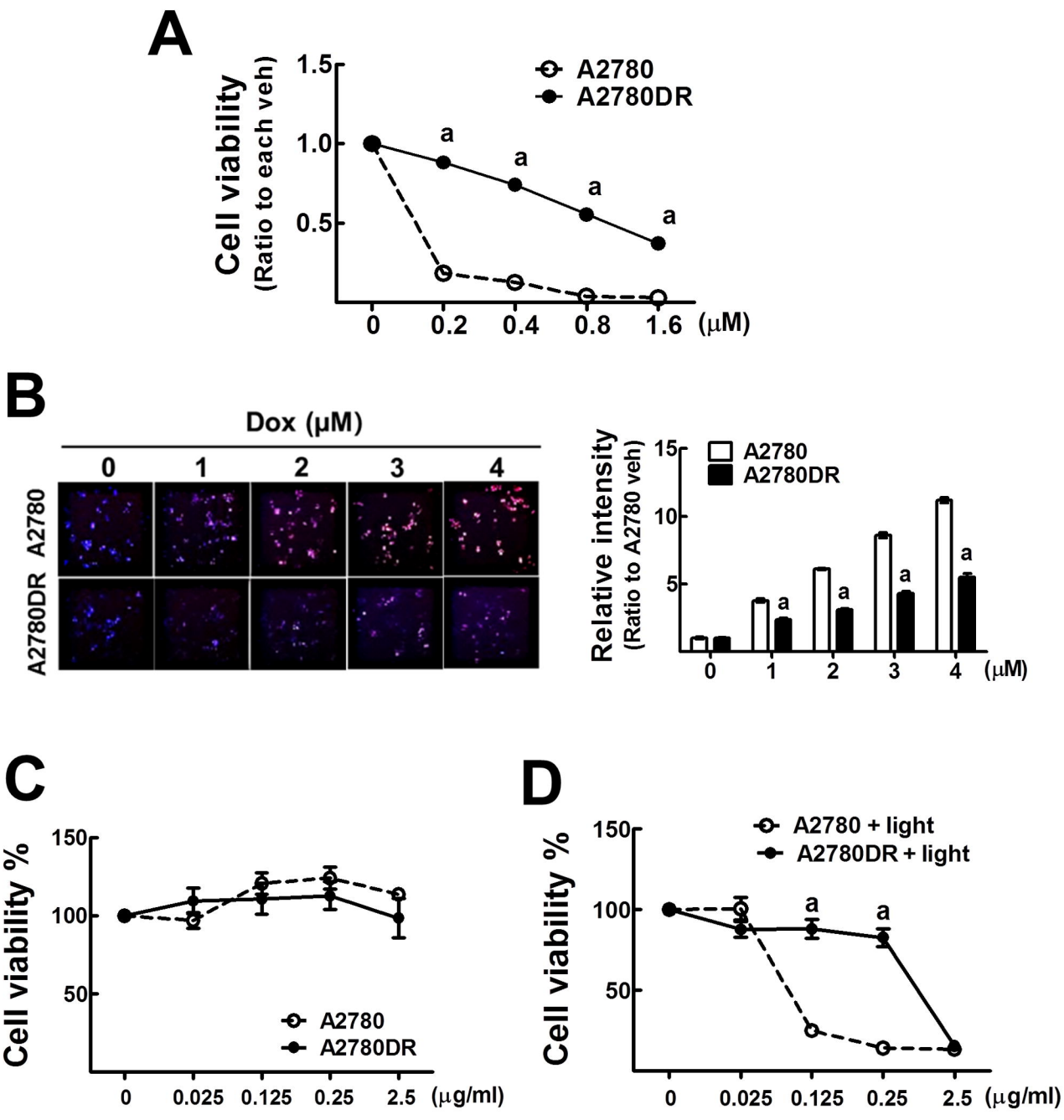
A
Cell viability
(Ratio to each veh)
1.5
1.0
0.5
A2780
A2780DR
a
a
a
a
0
0.2
0.4
0.8
1.6
(μM)
B
Dox (μM)
0
1
2
3
4
A2780
A2780DR
Relative intensity
(Ratio to A2780 veh)
15
10
5
A2780
A2780DR
a
a
a
a
0
1
2
3
4
(μM)
C
Cell viability %
150
100
50
A2780
A2780DR
0
0.025
0.125
0.25
2.5
(μg/ml)
D
Cell viability %
150
100
50
A2780 + light
A2780DR + light
a
a
0
0.025
0.125
0.25
2.5
(μg/ml)

Fig. 1

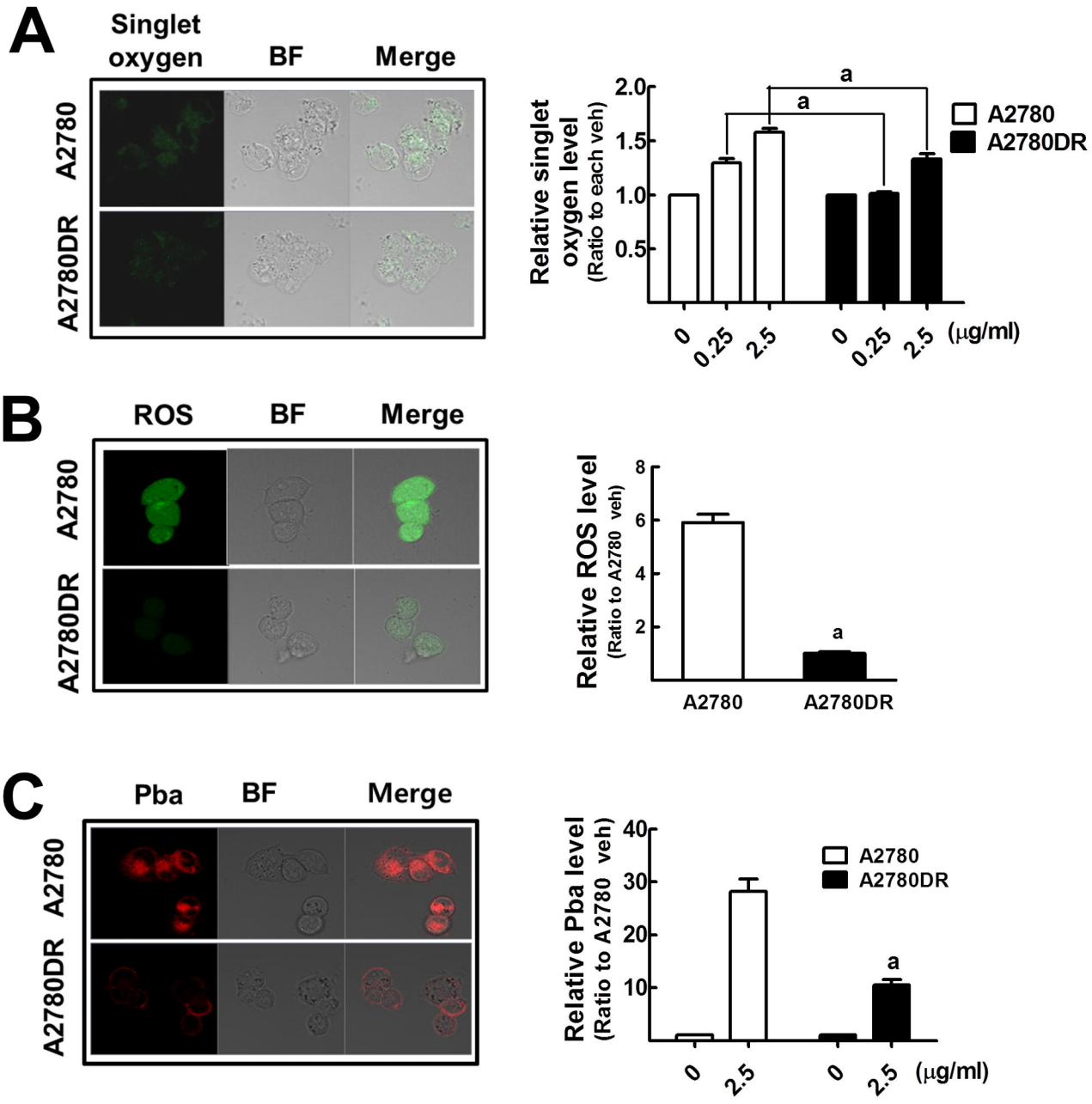
A
Singlet oxygen
BF
Merge
A2780
A2780DR
Relative singlet oxygen level
(Ratio to each veh)
2.0
1.5
1.0
0.5
a
a
A2780
A2780DR
0
0.25
2.5
0
0.25
2.5
(μg/ml)
B
ROS
BF
Merge
A2780
A2780DR
Relative ROS level
(Ratio to A2780 veh)
8
6
4
2
a
A2780
A2780DR
C
Pba
BF
Merge
A2780
A2780DR
Relative Pba level
(Ratio to A2780 veh)
40
30
20
10
A2780
A2780DR
a
0
2.5
0
2.5
(μg/ml)

Fig. 2

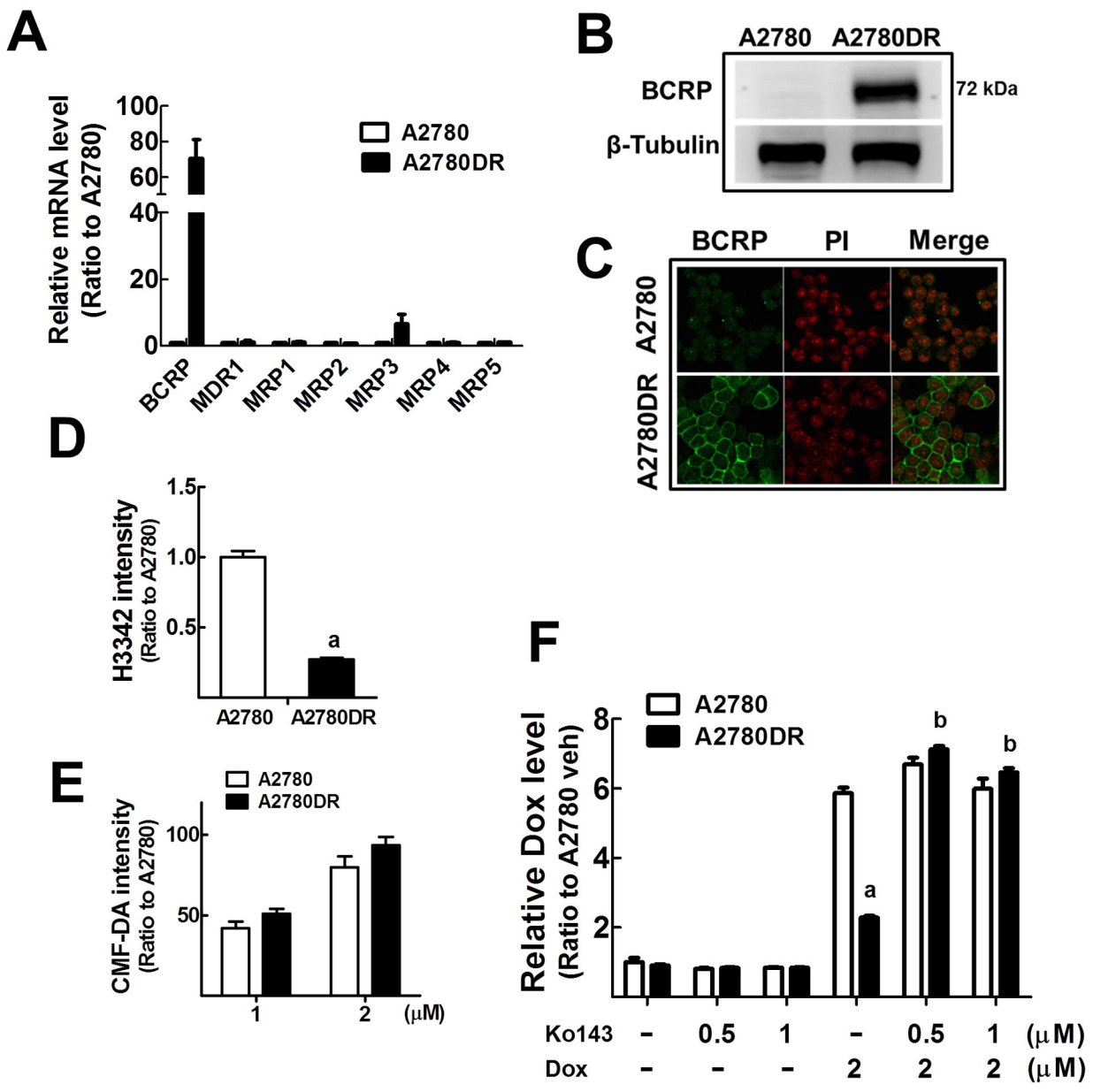
A
Relative mRNA level
(Ratio to A2780)
100
80
60
40
20
0
A2780
A2780DR
BCRP
MDR1
MRP1
MRP2
MRP3
MRP4
MRP5
B
A2780
A2780DR
BCRP
β-Tubulin
72 kDa
C
BCRP
PI
Merge
A2780
A2780DR
D
H3342 intensity
(Ratio to A2780)
1.5
1.0
0.5
a
A2780
A2780DR
E
CMF-DA intensity
(Ratio to A2780)
A2780
A2780DR
100
50
1
2
(μM)
F
Relative Dox level
(Ratio to A2780 veh)
A2780
A2780DR
8
6
4
2
a
b
b
Ko143 - 0.5 1 - 0.5 1 (μM)
Dox - - - 2 2 2 (μM)

Fig. 3

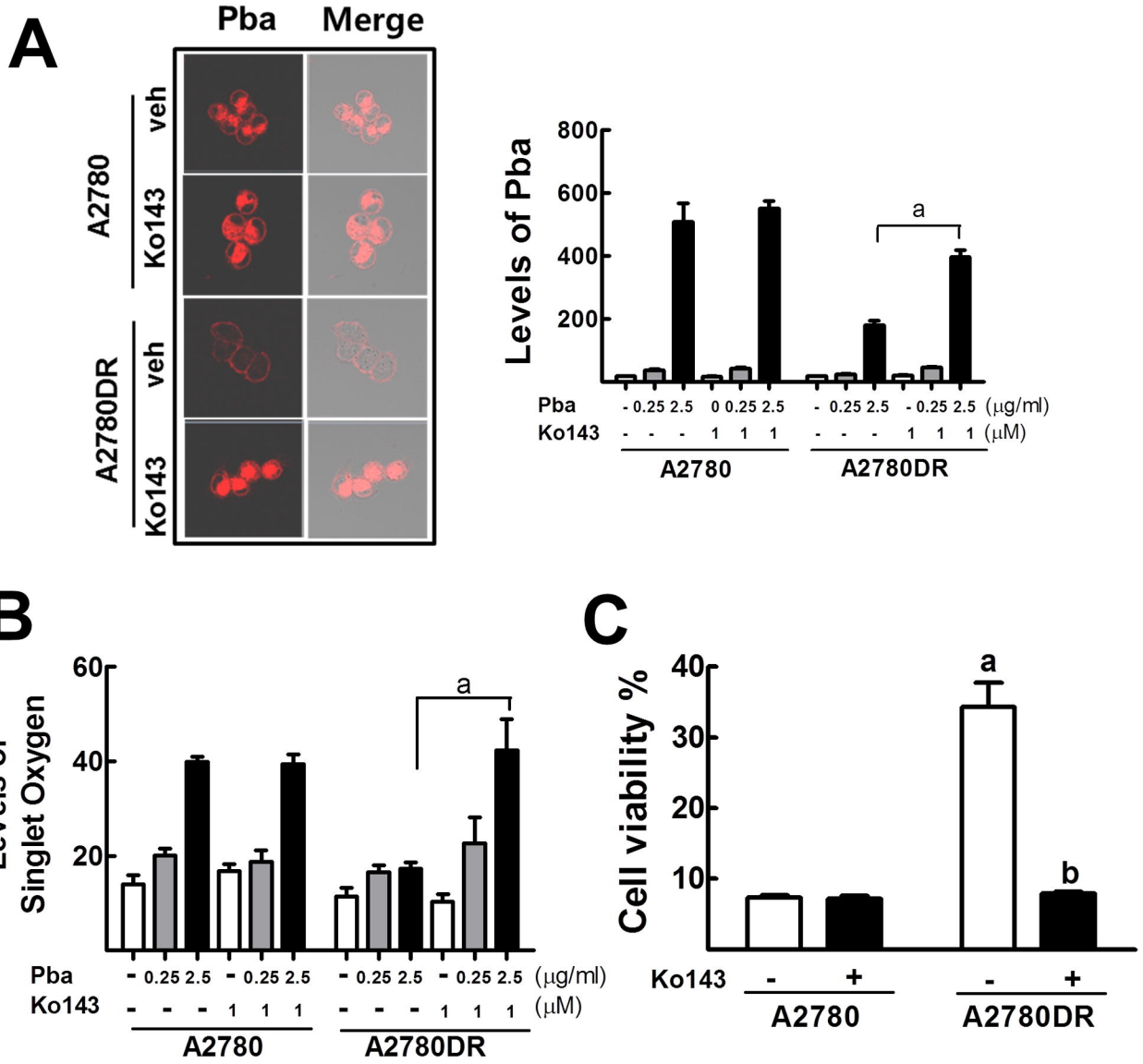
A
Pba
Merge
A2780
veh
Ko143
A2780DR
veh
Ko143
Levels of Pba
800
600
400
200
a
Pba - 0.25 2.5 0 0.25 2.5 - 0.25 2.5 - 0.25 2.5 (μg/ml)
Ko143 - - - 1 1 1 - - - 1 1 1 (μM)
A2780
A2780DR
B
Levels of Singlet Oxygen
60
40
20
a
Pba - 0.25 2.5 - 0.25 2.5 - 0.25 2.5 - 0.25 2.5 (μg/ml)
Ko143 - - - 1 1 1 - - - 1 1 1 (μM)
A2780
A2780DR
C
Cell viability %
40
30
20
10
a
b
Ko143 - + - +
A2780
A2780DR

Fig. 4

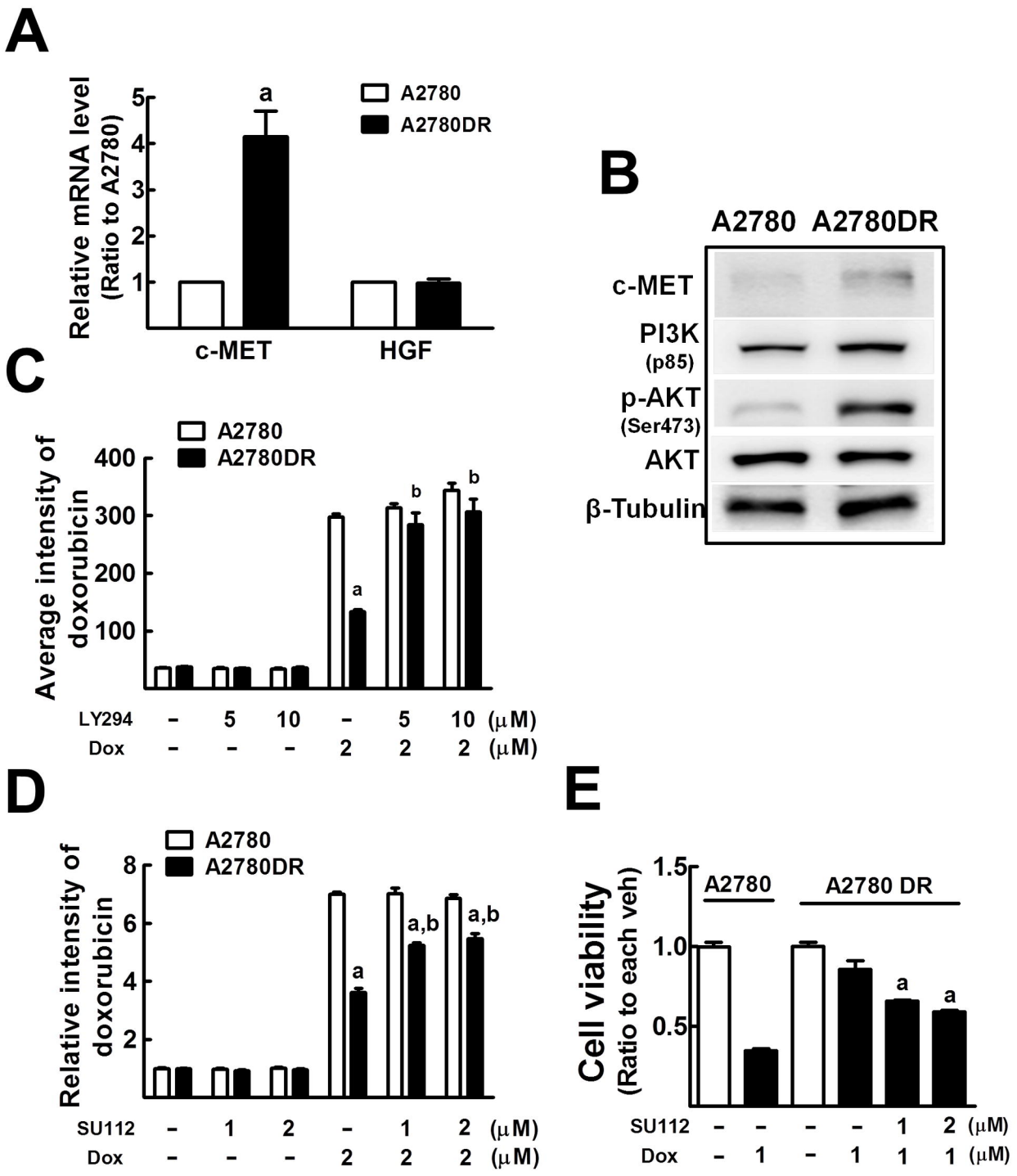
A
Relative mRNA level (Ratio to A2780)
A2780
A2780DR
a
c-MET
HGF
B
A2780
A2780DR
c-MET
PI3K (p85)
p-AKT (Ser473)
AKT
β-Tubulin
C
Average intensity of doxorubicin
A2780
A2780DR
LY294
Dox
(μM)
D
Relative intensity of doxorubicin
SU112
Dox
E
Cell viability (Ratio to each veh)
A2780
A2780 DR
SU112
Dox

Fig. 5

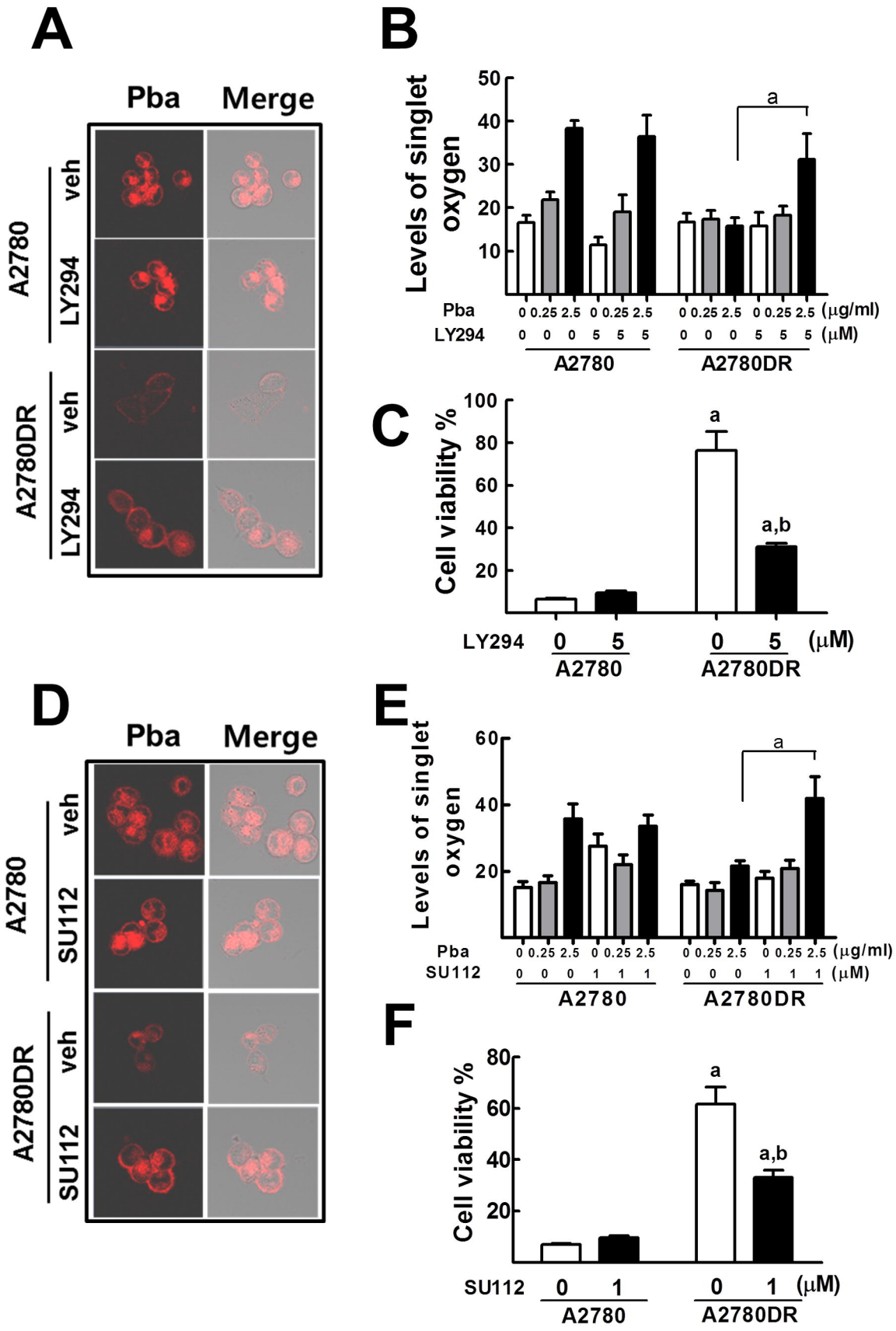
A
Pba
Merge
A2780
veh
LY294
A2780DR
veh
LY294
B
Levels of singlet oxygen
50
40
30
20
10
a
Pba
0 0.25 2.5 0 0.25 2.5 0 0.25 2.5 0 0.25 2.5 (μg/ml)
LY294
0 0 0 5 5 5 0 0 0 5 5 5 (μM)
A2780
A2780DR
C
Cell viability %
100
80
60
40
20
a
a,b
LY294
0 5 0 5 (μM)
A2780
A2780DR
D
Pba
Merge
A2780
veh
SU112
A2780DR
veh
SU112
E
Levels of singlet oxygen
60
40
20
a
Pba
0 0.25 2.5 0 0.25 2.5 0 0.25 2.5 0 0.25 2.5 (μg/ml)
SU112
0 0 0 1 1 1 0 0 0 1 1 1 (μM)
A2780
A2780DR
F
Cell viability %
80
60
40
20
a
a,b
SU112
0 1 0 1 (μM)
A2780
A2780DR

Fig. 6

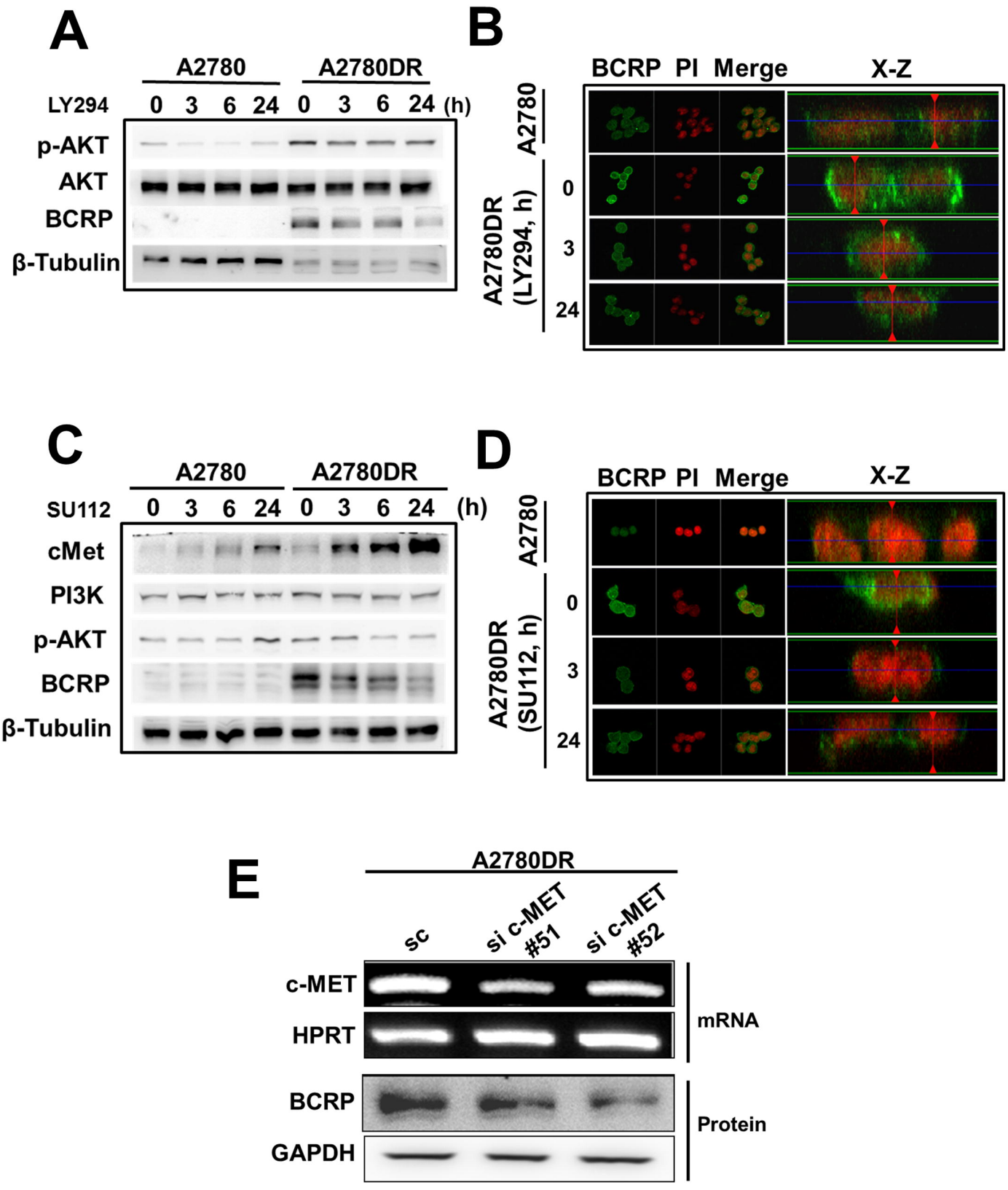
A
A2780
A2780DR
LY294
0 3 6 24 0 3 6 24 (h)
p-AKT
AKT
BCRP
β-Tubulin
B
BCRP PI Merge
X-Z
A2780
A2780DR (LY294, h)
0
3
24
C
A2780
A2780DR
SU112
0 3 6 24 0 3 6 24 (h)
cMet
PI3K
p-AKT
BCRP
β-Tubulin
D
BCRP PI Merge
X-Z
A2780
A2780DR (SU112, h)
0
3
24
E
A2780DR
sc
si c-MET #51
si c-MET #52
c-MET
HPRT
mRNA
BCRP
GAPDH
Protein

Fig. 7

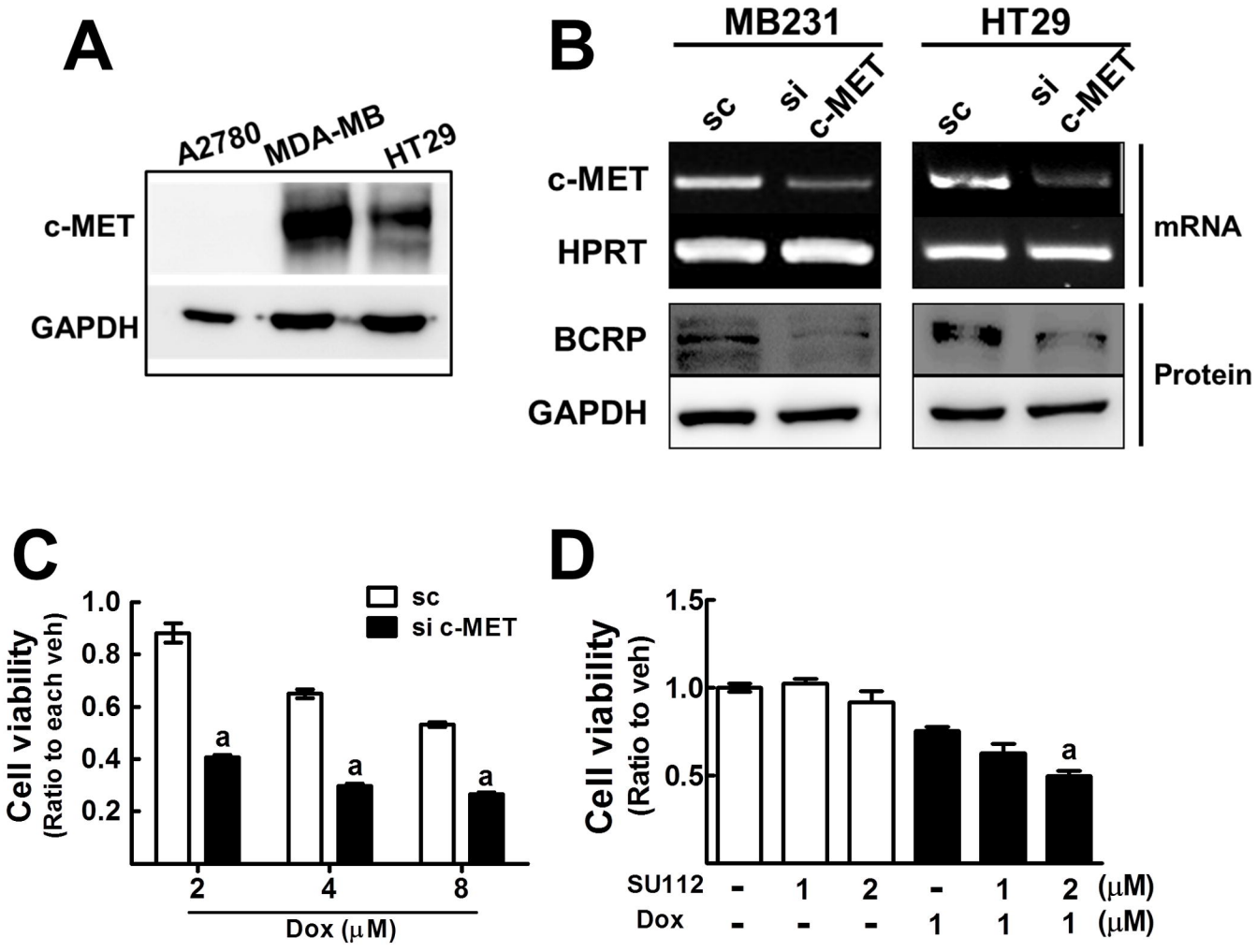
A
A2780
MDA-MB
HT29
c-MET
GAPDH
B
MB231
HT29
sc
si
c-MET
c-MET
HPRT
BCRP
GAPDH
mRNA
Protein
C
Cell viability
(Ratio to each veh)
1.0
0.8
0.6
0.4
0.2
sc
si c-MET
a
2
4
8
Dox (μM)
D
Cell viability
(Ratio to veh)
1.5
1.0
0.5
a
SU112 - 1 2 - 1 2 (μM)
Dox - - - 1 1 1 (μM)

Fig. 8